Atmos. Chem. Phys. Discuss., https://doi.org/10.5194/acp-2018-367
Manuscript under review for journal Atmos. Chem. Phys.
Discussion started: 25 May 2018

Aerosol acidity in a megacity with high ambient temperature and relative humidity of Central China: temporal variation, determining factors and pollution transition effect

Mingming Zheng [1,2,3], Shaofei Kong [2*], Jianguo Bao [1*], Ke Xu [3], Shurui Zheng [2], Guowei Yang [2], Jihong Quan [3], Lianxin Yuan [3], Nan Chen [3], Yiping Tian [3], Huang Zheng [1,2], Jian Wu [1,2], Dantong Liu [4], Delong Zhao [5], Qin Yan [6], Tianliang Zhao [6], Shihua Qi [1]

1. Department of Environmental Science and Technology, School of Environmental Studies, China University of Geosciences (Wuhan), 430074, Wuhan, China

2. Department of Atmospheric Sciences, School of Environmental Studies, China University of Geosciences (Wuhan), 430074, Wuhan, China

3. Hubei Environment Monitoring Center, Wuhan, 430072, China

4. School of Earth, Atmospheric & Environmental Sciences, University of Manchester, UK

5. Beijing Weather Modification Office, Beijing 100089, China

6. Collaborative Innovation Center on Forecast and Evaluation of Meteorological Disasters, Nanjing University of Information Science and Technology, Nanjing 210044, China

Correspondence to: Shaofei Kong (kongshaofei@cug.edu.cn) or Jianguo Bao (bjianguo888@126.com)

Atmos. Chem. Phys. Discuss., https://doi.org/10.5194/acp-2018-367
Manuscript under review for journal Atmos. Chem. Phys.
Discussion started: 25 May 2018

Abstract: Aerosol acidity affects the chemical transformation of aerosols and subsequent haze formation. High resolution (1-h) observation of water-soluble inorganic ions in fine particles, gaseous pollutants, and meteorological parameters was conducted from September 2015 to August 2016 at Wuhan, a megacity of Central China with high relative humidity and ambient temperature, compared with north Chinese cities. By adopting thermodynamic model ISOROPPIA-Ⅱ, the aerosol acidity for different time scales, pollution episodes, and air mass directions was calculated. Aerosols in Wuhan were moderate acidic, with pH averaged as 3.30 ± 0.49. The aerosol acidity was higher in July (pH as 2.64 ± 0.31), September (pH as 2.75 ± 0.30) and August (pH as 2.79 ± 0.29), and lower in January (pH as 3.77 ± 0.28) and March (pH as 3.70 ± 0.16). It decreased with the air pollution increasing, with the pH values of 3.07 ± 0.45, 3.63 ± 0.27 and 3.84 ± 0.22 for clean, transition and polluted episodes, respectively. The air masses in Wuhan transported from North China exhibited higher aerosol acidity, with pH averaged as 3.17-3.22. The unique environmental and meteorological conditions (high humidity, annual averaged RH as 0.74 ± 0.13) lead to excess ammonium (on average of 6.06 ± 4.51 μg m^{-3}) and abundant aerosol water content (AWC, on average of 71.0 ± 82.8 μg m^{-3}) in Wuhan, which can explain the lower $PM_{2.5}$ acidity in Wuhan than other megacities of China. At lower AWC level (less than ~15 μg m^{-3}), the particle pH showed a decreasing trend with AWC increased. When the AWC continuous increased from ~15 to ~380 μg m^{-3}, there was an obvious increase of particle pH. Then no significant growth of pH was found when AWC was higher than ~380 μg m^{-3}. With atmospheric RH increasing, the aerosol pH exhibited decreasing trend firstly and then increased, with the turning point RH as about 0.48. There was a logarithmic growth of aerosol pH with total NH_x (NH_3 + NH_4^+) increasing. From the fitted logarithmic curve, the aerosol pH of Wuhan was at the range of pH rapid growth stage with NH_x increasing, indicating that the control of ammonia emission in Wuhan could be an effective way to reduce the aerosol pH and further mitigate air pollution. This paper firstly obtained the aerosol acidity properties at a megacity under abundant ammonium and high humidity with high time-resolution, which is an important supplementary for the current aerosol acidity research around the world.

Keywords: water-soluble inorganic ions; aerosol acidity; high time-resolution; pollution episodes; aerosol water content; excess ammonium

Atmos. Chem. Phys. Discuss., https://doi.org/10.5194/acp-2018-367
Manuscript under review for journal Atmos. Chem. Phys.
Discussion started: 25 May 2018

1 Introduction

Aerosol acidity is one of the key factors affecting the organic (Jang et al., 2002; Surratt et al., 2007; Cao and Jang, 2010; Pathak et al., 2011) and inorganic secondary aerosol formation (Underwood et al., 2001; Manktelow et al., 2010; Wang et al., 2016a), by gas-aerosol partitioning (Grassian, 2001; Keene et al., 2004), acid-catalyzed heterogeneous reaction (Jang et al., 2002; Nemitz et al., 2004; Xu et al., 2015a) and migration of redox minerals and metals (Meskhidze et al., 2003), etc. Acidic aerosols have the capability to reduce atmospheric visibility (Watson, 2002), disturb atmospheric radiative balance (Crumeyrolle et al., 2008), threaten human health and deteriorate ecosystems (Schindler, 1988; Larssen et al., 2006; Johnson et al., 2008). Recently, aerosol acidity has raised wide attention and controversy in view of its vital role in haze formation of China (Liu et al., 2017; Tian et al., 2018; Zhou et al., 2018).

The aerosol acidity exhibited spatiotemporal discrepancy, owing to the diversities of source emission and meteorological conditions. Currently, the research of aerosol acidity in China is becoming a hotspot, with studies mainly concentrated in northern cities like Beijing (He et al., 2012; Yang et al., 2015; Cheng et al., 2016; Wang et al., 2016a), eastern coastal cities like Shanghai (Pathak et al., 2009), southern coastal cities including Guangzhou (Huang et al., 2011) and Hongkong (Pathak et al., 2003; Pathak et al., 2004a; Yao et al., 2006; Yao et al., 2007), and western cities of Chongqing (He et al., 2012) and Lanzhou (Pathak et al., 2009). One study has been conducted at a background mountainous site (Zhou et al., 2012). In general, aerosol acidity in China was lower than those in Europe (Bougiatioti et al., 2016) and United States (Weber et al., 2016). He et al. (2012) indicated that the aerosol acidity in North China was lower than that in the south. Even in the same city, the aerosol acidity was different. He et al. (2012) observed that fine particles ($PM_{2.5}$) in Beijing was strong acidic with pH ranging in 0-3; Liu et al. (2017) calculated the pH value of $PM_{2.5}$ in Beijing as about 4.2; Wang et al. (2016a) indicated that $PM_{2.5}$ in Beijing was completely neutralized with pH as about 7. One of the key factors for these diversities is that these studies were done at a given period with different pollution levels. Liu et al. (2017) found that along with the pollution levels increased, the aerosol pH values decreased for a typical haze formation processes in Beijing. Former researchers highlighted the importance to obtain the aerosol acidity under different time scales and different pollution episodes, which is important to better identify the formation mechanism of air pollution at a certain region. Till now, few studies were reported to

analyze the aerosol acidity for a long-time period, owing to the absence of online high-resolution dataset for gaseous pollutants and ionic components synchronously. It may limit the understanding of how the aerosol acidity affects the atmospheric chemistry, in view of a pollution transition event, monthly variation and diversities for different air mass trajectories.

The molar ratio of cations to anions is always used to estimate aerosol acid-alkaline property qualitatively (Yao et al., 2006; Hennigan et al., 2015; Wang et al., 2016a), depending on the selected ionic species (He et al., 2012). Thermodynamic models such as ISORROPIA (Nenes et al., 1998; Fountoukis and Nenes, 2007), E-AIM (Carslaw et al., 1995; Clegg et al., 1998; Friese and Ebel, 2010) and SCAPE (Meng et al., 1995) were developed and widely adopted to calculate aerosols acidity quantitatively, with outputs of pH, [H^+] and aerosol water content (AWC), though inherent imperfect existed for these models (Wang et al., 2018).

AWC exerts a driving role in the variation of aerosol acidity (Liu et al., 2017). Zhou et al. (2012) indicated high water content can cause HSO_4^- dissociating to form free H^+ when RH > 0.65. In addition, AWC serves as a medium for aqueous phase reaction of SO_2 oxidation (Pilinis et al., 1989; Ervens et al., 2011; Cheng et al., 2016), which can also lead to the increase of aerosol acidity (Seinfeld et al., 2006). However, high water content of aerosols in return may dilute the hydrogen ion concentrations and increase pH value. Guo et al. (2015) showed that the diurnal variation of pH was mainly driven by AWC dilution. It was observed that the temporal trends of particle pH were in accordance with AWC rather than H^+, and the aerosol acidity added with the decrease of AWC in Beijing, despite the decreasing of H^+ (Liu et al., 2017). AWC was not only closely associated with atmospheric relative humidity (RH) and temperature (Temp) (Guo et al., 2015), but also well correlated with secondary inorganic salt (Cheng et al., 2016) which will again assimilate more water because of hygroscopicity (Engelhart et al., 2011; Bian et al., 2014). So is there an inflection point of AWC between the promoting role through the aqueous phase formation and the inhibition role by the dilution effect on the acidic inorganic ions under a specific circumstance? Till now, as obvious studies are always conducted in a limited season or pollution episodes (Zhou et al., 2012; Bian et al., 2014; Guo et al., 2015; Cheng et al., 2016; Wang et al., 2016a; Liu et al., 2017; Wang et al., 2018), no studies have listed observed evidence directly to answer this question.

Except for AWC, ammonia and ammonium were also regarded as determining factors on aerosol acidity (Liu et al., 2017), which were the main species to neutralize acid (Sun and Wexler,

1998; Wang et al., 2015). The ammonium-to-sulfate ratio was used to describe the ammonium-rich or ammonium-poor conditions (Pathak et al., 2004a; Huang et al., 2011; Kumar and Sunder Raman, 2016), with the ratio higher than 1.5 implying an ammonia rich atmosphere (Kumar and Sunder Raman, 2016). Pathak (2004) indicated that pH increased with increasing ammonium-to-sulfate ratio. The correlation of NH_4^+ with SO_4^{2-} and NO_3^- also can be used to judge the ammonia rich or poor status (Kumar and Sunder Raman, 2016). Recently, Liu et al. (2017) concluded that the excess ammonia resulted in the pH increasing by logarithm growth form in north China. Under ammonia-rich air, positive correlation between excess NH_4^+ and NO_3^- was found (Pathak et al., 2009). Therefore, for the regions with abundant agricultural activities which are the main emission sources for ammonia, the relationship of ammonia, aerosol acidity and air pollution needs a clear illustration.

Wuhan and its surrounding cities (WSC) belong to the key regions in the State Council's Action Plan on Prevention and Control of Atmospheric Pollution (Figure 1a). WSC has become the most polluted region with high $PM_{2.5}$ concentrations except for the regions of Beijing-Tianjin-Hebei (Qi et al., 2017; Gao et al., 2018), Yangtze River Delta (Shen et al., 2015; Chen et al., 2017) and Sichuan Basin (Wang et al., 2017a; Ning et al., 2018) (Figure 1b). Meanwhile, as WSC is located in the center of China, the air masses from other different polluted regions all can impact the aerosol concentrations and compositions. At the west of WSC, there locates JiangHan Plain (JHP) which is a key food-cotton base of China. The WSC and surrounding JHP hold high ammonium emission intensity (Huang et al., 2012; Xu et al., 2015b; Wang et al., 2018). At the northeast and northwest of WSC, there locates TongBai Mountain and DaBie Mountain (Figure 1c), which directly decided the transportation routes of air masses in cold period from North China Plain when the north winds dominated (Figure 1b). Wuhan belongs to subtropical monsoon climate, and owns hundreds of lakes (Figure 1d), which lead to its higher ambient temperature and atmospheric relative humidity (RH). The unique geographical, emission and meteorological conditions implied that the aerosol acidity and its role in air pollution transition should be quite different from other regions, especially for the recently studied cities in North China. Meanwhile, the high RH (annual mean 0.74, in this research, all the $PM_{2.5}$ compositions and meteorological data for rainy day were excluded), temperature (annual mean 292.2K) and serious air pollution in Wuhan provide an ideal site to identify how the RH, AWC and precursor gases affect aerosol acidity.

Therefore, based on one-year continuous observation of hourly water-soluble inorganic ions in

$PM_{2.5}$ and precursor gases from September 2015 to August 2016, $PM_{2.5}$ acidity was calculated by thermodynamic model ISOROPPIA-Ⅱ. The variation of acidity in different months, pollution episodes and for different air mass transportation directions were discussed and possible reasons were investigated. The results are urgently and helpful to understand the relationship of chemical composition-aerosol acidity-air pollution in different time scales and to enrich the formation mechanism of serious air pollution out of North China Plain.

2 Method and modeling

2.1 Sampling and instrumentation

The observation site (30.53° E, 114.36° N) located in the city center (Figure 1d). It is about 20 m above ground and surrounded by commercial/residential mixed area with no obvious industrial sources. Water-soluble ions (WSI) including SO_4^{2-}, NO_3^-, Cl^-, NH_4^+, Na^+, K^+, Ca^{2+} and Mg^{2+} in $PM_{2.5}$ and atmospheric NH_3, HCl, HNO_3, and HNO_2 were synchronously measured by an online ion chromatography analyzer with one-hour resolution by Marga ADI 2080 (Monitor for Aerosols and Gases in Ambient Air). The detailed description of the equipment can be found in previous studies (Rumsey et al., 2014). One-year continuous monitoring was done from September 2015 to August 2016, except data missing due to equipment maintain in February. Concurrently, hourly $PM_{2.5}$, O_2, SO_2, NO_2, and O_3 were observed by automatic on-line monitoring instrument, with the methods of β-ray, ultraviolet fluorescence, chemiluminescence and ultraviolet absorption, respectively. The synchronous meteorological data including relative humidity (RH) and temperature (Temp) were obtained from local meteorological observatory. Ionic equivalent ratio was employed to a preliminary qualitative estimation of the particle neutralization and acidity. The ratio of total cations and anions were calculated as following (Zhang et al., 2007; Tanner et al., 2009; Hennigan et al., 2015):

$$Cation / Anion = \left(NH_4^+ + 2*Ca^{2+} + Na^+ + 2*Mg^{2+} + K^+\right) / \left(2*SO_4^{2-} + NO_3^- + Cl^-\right) \quad (1)$$

2.2 Fine particle acidity calculation

Thermodynamic model ISOROPPIA-Ⅱ (http://nenes.eas.gatech.edu/ISORROPIA) was employed to calculate in-situ aerosol acidity. It can predict which species exist in the gas or aerosol phase and can calculate their concentrations at chemical equilibrium status, including H^+, water content and aerosol pH, with the inputs of SO_4^{2-}, NO_3^-, NH_4^+, Cl^-, K^+, Ca^{2+}, Na^+, and Mg^{2+}, as well

as temperature and relative humidity. In this study, the forward mode with metastable state was adopted as its better performance (Fountoukis and Nenes, 2007; Guo et al., 2015; Hennigan et al., 2015; Guo et al., 2016; Weber et al., 2016). Well correlations between the predicted and observation data were found in Figure 2.

2.3 Trajectory clustering

Backward trajectory analysis by HYSPLIT model (Version 4) was used to explore the influence of air masses originated from different directions on the aerosol acidity of Wuhan. 72 h backward trajectories were calculated for 4 times each day (00:00, 06:00, 12:00 and 18:00), with the starting height at 200 m above ground. The input meteorological data was in 6-h hourly resolution acquired from NOAA/ARL. The trajectories were clustered by the clustering analysis procedure provided in the HYSPLIT user's guide.

3 Results and discussions

3.1 General characteristic of WSI in Wuhan

As listed in Table 1, the annual average mass concentration of $PM_{2.5}$ in Wuhan was 63.4 ± 35.2 μg m^{-3}, exceeding the annual average secondary standard of China Ambient Air Quality (35 μg m^{-3}). $PM_{2.5}$ showed the maximum concentration in winter (92.6 ± 45.6 μg m^{-3}) and the minimum value in summer (37.3 ± 12.0 μg m^{-3}), which was consistent with former researches. Total WSI concentrations accounted for 70% of $PM_{2.5}$ mass concentration on average, also higher in winter and lower in summer.

The dominated ions were SO_4^{2-}, NO_3^- and NH_4^+ (SNA), with a proportion up to 91-93% and 55-73% in total ions and $PM_{2.5}$, respectively. The ratios of SNA to $PM_{2.5}$ in Wuhan were higher than those in urban sites of Beijing (28%) (Zheng et al., 2005), Chongqing (30%) (He et al., 2012), Shanghai (36%) and Guangzhou (27%) (Yang et al., 2011). The high relative humidity in Wuhan (annual average as 0.74) may be one of the key factors. SO_4^{2-} production can increase along with RH increasing due to the aerosol hygroscopicity and aqueous phase oxidation (Wang et al., 2016a). The SNA concentrations were highest in winter (61.1 ± 35.1 μg m^{-3}) and lowest in summer (24.6 ± 12.7 μg m^{-3}), then followed by spring (43.4 ± 21.0 μg m^{-3}) and fall (32.4 ± 14.2 μg m^{-3}). It was different from the results in North China Plain (NCP), Sichuan Basin (SB), Yangtze River Delta and Pearl River Delta (Fu et al., 2016), where the lowest SNA proportions were found in spring or fall. The meteorological condition and precursor emissions, can explain the seasonal variation pattern

(Fu et al., 2016). Although there was higher sulfate formation rate in summer in Wuhan, the SO_2 in summer was low to 4.7 μg m^{-3} (Table 2). The low SNA concentrations in summer were mainly related to the lower nitrate and ammonium formation rate (Table 2) and high atmospheric boundary layer height (Figure 4a).

NO_3^- concentrations exhibited the highest concentration in winter (25.3 μg m^{-3}) and the lowest in summer (5.6 μg m^{-3}), with winter/summer ratio of 4.5. SO_4^{2-} concentrations also exhibited the same seasonal variation. Lower sulfate concentration in summer was contrary to previous studies (Tai et al., 2010; Yang et al., 2011; Hand et al., 2012), which indicated that strong atmospheric oxidation (higher O_3 concentration in summer), higher temperature and relative humidity were beneficial to sulfate formation from SO_2. While in this study with lower precursor concentration and higher boundary layer height, relatively low concentrations of sulfate and nitrate in summer were found in Wuhan.

The averaged NH_4^+ mass concentration was 10.4 μg m^{-3}, higher than those in Beijing (7.4 μg m^{-3}) (He et al., 2012), Chongqing (7.9 μg m^{-3}) (He et al., 2012), Guangzhou (5.2 μg m^{-3}) (Lai et al., 2016), Shanghai (6.0 μg m^{-3}) (Wang et al., 2016b), Tianjin (6.9 μg m^{-3}) (Shi et al., 2017) and Xi′an (7.6 μg m^{-3}) (Wang et al., 2014). NH_4^+ exhibited higher concentrations in winter (15.4 ± 8.9 μg m^{-3}) and lower concentrations in summer (6.81 ± 3.42 μg m^{-3}) in Wuhan. The reason may be that under high temperature and strong solar insolation in summer, ammonium preferred to exist in the form of gas phase due to the thermal equilibrium. Strong correlation was found between NO_3^- and NH_4^+ ($R^2 = 0.94$, $p < 0.05$), as well as SO_4^{2-} and NH_4^+ ($R^2 = 0.92$, $p < 0.05$), implying that $(NH_4)_2SO_4$ and NH_4NO_3 could be the main existing forms in $PM_{2.5}$ of Wuhan, similar to former cities (Han et al., 2016).

Other species including K^+, Ca^{2+}, Na^+, Mg^{2+}, and Cl^- constituted a minor fraction, totally accounting for 7-9% of total ions. The Cl^- concentration was higher, and subsequently followed by K^+, Ca^{2+}, Na^+, and Mg^{2+}. Higher Cl^- concentrations were measured in winter (2.87±1.25 μg m^{-3}), approximately two or three times than those in other seasons. The Na^+/Cl^- ratio in winter (0.09) was obviously lower than that of seawater (0.557) (Hegde et al., 2016), reflecting the dominance of other sources for Cl^- instead of sea salt. The weak correlation ($R^2 = 0.20$, $p < 0.05$) between Cl^- and Na^+ verified this. Furthermore, Cl^- was positively ($p < 0.05$) correlated with NO_3^- ($R^2 = 0.78$), SO_4^{2-} ($R^2 = 0.55$), NH_4^+ ($R^2 = 0.71$) and K^+ ($R^2 = 0.59$), which were mainly derived from anthropogenic

emissions. Therefore, Cl^- was inferred to be associated with regional transport of domestic coal and biofuel combustion emission for heating from North China (Yin et al., 2014). The dominated north wind in Wuhan at winter favored it (Figure 4).

K^+ in Wuhan was not abundant compared with those in Shanghai (Wang et al., 2016b), Beijing (Han et al., 2016) and coastal areas (Yin et al., 2014). It was moderately correlated with NO_3^- (R^2 = 0.64, p <0.05), SO_4^{2-} (R^2 = 0.62, p <0.05), NH_4^+ (R^2 = 0.63, p <0.05) and Cl^- (R^2 = 0.59, p <0.05), indicating homology source of them. The highest K^+ in winter of Wuhan can be related to the wood burning (Fourtziou et al., 2017) for domestic heating in NCP (Zhang et al., 2017; Zhu et al., 2017). High intensity discharge of K^+ from fireworks and crackers in Spring Festival periods could not be ignored, which usually occurred in January or February (Kong et al., 2015).

Ca^{2+} was commonly derived from soil or crustal dust and construction activities (Hegde et al., 2016). Ca^{2+} in Wuhan showed slightly higher value in winter and spring than those in summer and fall, similar to previous studies (Zhao et al., 2010; He et al., 2012). Ca^{2+} was only significantly correlated with Mg^{2+} (R^2 = 0.80, p < 0.05). Different from Beijing (Han et al., 2016) and Xi' an (Wang et al., 2014), no correlations for Ca^{2+}-NO_3^-, Ca^{2+}-SO_4^{2-}, Mg^{2+}-NO_3^- and Mg^{2+}-SO_4^{2-} were found in Wuhan, indicating different atmospheric chemical processes between northern and central Chinese cities. In north China, the mineral dust fraction of $PM_{2.5}$ was higher (Tao et al., 2017), and was involved in atmospheric processes by internally mixing with secondary aerosols (Cheng et al., 2016; Wang et al., 2017b).

3.2 Aerosol acidity in Wuhan

Figure 3a shows the daily variation of $PM_{2.5}$ aerosol acidity in Wuhan. The daily pH values ranged between 2.21 – 4.19, with an average of 3.30, indicating moderate acidic in Wuhan. The lowest pH value occurred in summer, averaged as about 2.84. The pH values in winter were higher as about 3.71. The AWC in autumn, winter, spring, and summer were 66.9, 118.5, 66.5 and 36.2 μg m^{-3}, respectively, which can explain the seasonal variation of pH values primarily. There is a double effect of AWC on aerosol pH, including the enhancement of bisulfate dissociation to form free H^+ through the hydrolysis process and dilution effects of proton concentrations in droplets (Pathak et al., 2004a; Zhou et al., 2012). At higher RH, the dilution effect on the molarity of acidic species was more important than H^+ releasing from bisulfate (Pathak et al., 2004a). Previous studies showed that aerosol pH varied in consistency with AWC (Liu et al., 2017). From September to January, the

aerosol pH gradually increased from 2.75 to 3.77 (Figure 5) along with the increasing of AWC, which buffered the aerosol acidity. From May to August, when AWC decreased from 80.8 to 32.4 μg m^{-3}, the pH decreased 0.65 units from 3.44 to 2.79. The H^+ concentrations generally exhibited an opposite variation of pH value except for November when more H^+ did not result in lower pH value (3.53) because of higher AWC (151.7 μg m^{-3}).

The ratios of cations to anions were also listed in Figure 3(c). It could be found that there was no obvious relationship between pH and cations/anions ratios. The annual mean cations/anions ratio was near unity (1.10), reflecting completely neutralized, which was not in accordance with the prediction by thermodynamic models. It might be resulted from the negligence in considering the particle liquid water and dissociation state of individual ion (Guo et al., 2015). Thus, ionic molar ratios could not be the proxy for discussing aerosol acidity.

Table 3 compared the aerosol acidity of Wuhan with other cities. Aerosols mostly exhibited acidic around the world. Particle pH in Wuhan was higher than most of the other cities. As discussed above, the specific climate, geography, and emissions may explain it. Besides, aerosol acidity was dynamically changing. The particle pH increased in last decade of Beijing as Table 3 shown, which might be due to the increase of atmospheric NH_3 and decreasing of SO_2 (Meng et al., 2011; Liu et al., 2013). Detailed discussion about the key impacting factors on aerosol acidity is listed below.

3.3 Key driving factors for aerosol acidity variation

As mentioned above, AWC exerted an important role in aerosol acidity variation. Figure 6a exhibited the relationship between pH with AWC. From the fitting curve, the particle pH firstly showed a decreasing trend with AWC increased under much lower AWC level (less than about 15 μg m^{-3}). Then, with the AWC increasing from ~15 to ~380 μg m^{-3}, the dilution effect on aerosol acidity gradually dominated, which offset or even surpass the liquid-phase reaction and formation of secondary inorganic ions, causing the obvious and quick increase of particle pH. The SNA contents exhibited its peak value when the AWC increased to about 380 μg m^{-3}, then with the AWC increasing, SNA contents decreased (Figure 6d). When AWC > 380 μg m^{-3}, along with the increasing of AWC, a slowly increasing and gradually no significant growth of pH was found.

It was favored by the SNA-RH correlation coefficient variations with RH increasing (Figure 7b) and relationship of AWC-RH (Figure 7c), SNA-AWC (Figure 7d) and pH-RH (Figure 7e). Lower RH corresponded to lower AWC (Figure 7c). Under lower RH (< ~0.48) and AWC (< ~15 μg m^{-3})

values, the AWC dilution effect on aerosol acidity was negligible, and the dry particle quickly deliquesced and release H^+, resulting in the decrease of pH. The weaker or even negative correlation coefficient of SNA with RH was found when RH varied in 0.48- 0.75, accompanied with AWC and pH quick increasing, which reflected that the dominated role of dilution effects of AWC. As discussed above, SNA content reached its peak values when the AWC increased to about 380 μg m^{-3}, with corresponding RH as about 0.75-0.90, reflecting active liquid phase reaction, and resulting in buffering effect on pH increase. That might be the reason for the pH slowly growth when AWC was at ~380 μg m^{-3}. Then when RH was higher than 0.95, with the corresponding AWC was greater than 380 μg m^{-3}, obviously negative correlation between RH and SNA was obtained (R^2=0.59, $p < 0.05$), and it implied the dominated role of buffering effect of AWC, which lead to the continuously increasing of pH and gradually slowdown.

AWC is closely related to atmosphere temperature and relative humidity (RH) (Bian et al., 2014). High RH can facilitate the production of secondary inorganic salt, which will again assimilate more water because of hygroscopicity (Engelhart et al., 2011; Bian et al., 2014). However, in this study the RH was higher in July, August and September, while corresponding AWC were nearly the lowest (Figure 5), which may be resulted from the higher water evaporation from aerosol (Bougiatioti et al., 2016) due to the high temperature in summer period. It could be seen there was an exponential relationship between AWC and RH ($R^2 = 0.71$, $p < 0.05$) (Figure 6c). The correlation coefficient of atmospheric RH and fine particle pH in Wuhan was 0.39 ($p < 0.05$) by polynomial fitting (Figure 6e), showing that pH decreased with RH when RH was less than about ~0.48, and then pH increased with RH increasing when RH was higher than about 0.48. Atmospheric temperature can also pose impacts on AWC and pH (Figure 6f). Generally, lower temperature was corresponded to the higher AWC and pH values. When the temperature was higher than about 303 K (about 30 ℃), the AWC was all less than ~380 μg m^{-3}, and particles were more acidic. Figure 6e also showed that there were no obvious relations between SNA/$PM_{2.5}$ ratio with pH. It illustrated that the particle acidity or pH could be affected by other components except for inorganics, such as organics whose role in aerosol acidity can not be ignored (Wang et al., 2018).

Except for the AWC, RH and temperature, the excess ammonia or ammonium was also proved to affect aerosol acidity (Liu et al., 2017). Different from southeastern US (Weber et al., 2016) where the aerosols usually presented strong acid, the higher pH in this study was also likely related

with abundant ammonia and ammonium. As discussed above, the ammonium in Wuhan was at a higher level in China.

Ammonium was the primary basic species to neutralize acid (Seinfeld and Pandis, 2006) and it preferred to neutralize sulfate first, then reacted with nitrate when redundant, owing to the higher salting out efficiency of SO_4^{2-} than NO_3^- (Pathak et al., 2004a). A critical molar ratio of NH_4^+ to SO_4^{2-} was suggested as 1.5, implying SO_4^{2-} was completely neutralized and NO_3^- was stabilized by NH_4^+ (Pathak et al., 2004b; Huang et al., 2011). When the NH_4^+/SO_4^{2-} ratio was higher than 1.5, it indicated an ammonia rich atmosphere, and the excess NH_4^+ could be calculated as:

$$excess\ NH_4^+ = \left(\frac{[NH_4^+]}{[SO_4^{2-}]} - 1.5\right) * [SO_4^{2-}] \qquad (2)$$

In Figure 7a, the molar ratio of NH_4^+ to SO_4^{2-} in Wuhan mainly varied from 2:1 to 6:1, indicating that SO_4^{2-} was completely neutralized and mainly presented in the form of $(NH_4)_2SO_4$. Along with the increase of NH_4^+/SO_4^{2-} ratio, NO_3^- production increased, and it preponderated SO_4^{2-} formation The correlation coefficient between NH_4^+/SO_4^{2-} and NO_3^-/SO_4^{2-} in Wuhan was 0.85. In adequate ammonium condition, excess NH_4^+ was well correlated with NO_3^- (R^2 = 0.95) (Figure 7b), which was in consistency with previous studies (Pathak et al., 2009). The correlation of NH_4^+ with SO_4^{2-} and NO_3^- can also be used to judge the rich or poor status of NH_4^+, which was not obvious in poor NH_4^+ condition (Kumar and Sunder Raman, 2016). In Wuhan, the positive significant correlation between NH_4^+ vs SO_4^{2-} and NH_4^+ vs NO_3^- verified the NH_4^+ rich conditions. The excess ammonium may be in the form of NH_4Cl, with the high correlation between NH_4^+ and Cl^- (R^2 = 0.71).

Figure 8a showed the relationship between ammonium neutralized pH (with no excess NH_4^+ case) and pH variation (△pH, difference between the presence and absence of excess NH_4^+). The distinct negative correlation implied that higher aerosol acidity would be more susceptible by excess NH_4^+. Based on current excess NH_4^+ concentrations, simulating NH_4^+ decreased by 0.5, 1, 1.5, 2, 2.5 times of excess NH_4^+, and increased by 1, 2, 3, 4, 6, 8, 10, 12, 14, 16, 18, 20, 22, 24, 26, 28, 30, 35, 40, 45 and 50 times of excess NH_4^+. The predicted corresponding pH showed logarithmic growth with total NH_x (NH_3 + NH_4^+), implying that the pH increase insensitive gradually with NH_x increasing.

The NH_x concentrations of Wuhan were in the range of 2.27 - 48.3 μg m^{-3}, averaged as 19.2 μg m^{-3}, which still located in the range for the rapid growth stage of pH (Figure 8b). It was verified by

the positive relationship between △pH and the excess NH_4^+ ($R^2 = 0.45$, $p < 0.05$). However, it was different from the curve in Beijing which performed a logarithmic relationship (Liu et al., 2017). The same excess NH_4^+ concentrations in Beijing and Wuhan exhibited different stage of pH change, and higher excess NH_4^+ was afforded in Wuhan than Beijing for reaching the inflection point when the excess NH_4^+ increasing held little influence on pH change. Thus, it again confirmed that the aerosol acidity in Wuhan of Central China was impacted more by excess NH_4^+ than that of Beijing in North China. Wang et al. (2016a) indicated that the increase of pH value will promote precursor solubility and increase aqueous reaction rates, which will accelerate the formation of secondary inorganic salts and aggravate air pollution, resulting in more severe haze. Therefore, it should be emphasized that if the excess NH_4^+ in Wuhan was not controlled, the aerosol pH value will increase, which would worsen the air quality.

3.4 Aerosol acidity transition from clean to polluted periods

The visibility less than 5 km, 5-10 km and higher than 10 km were defined as polluted period, transition and clean period, respectively. The averaged visibility in Wuhan for the three episodes were 3.78 ± 0.96 km, 7.56 ± 1.59 km and 17.7 ± 5.71 km, with averaged $PM_{2.5}$ concentrations as 136.4, 85.0 and 45.9 μg m^{-3}, respectively. The average pH value at the clean stage was 3.07 ± 0.45, accompanied with low AWC (33.2 ± 42.9 μg m^{-3}), low excess NH_4^+ (3.70 ± 2.15 μg m^{-3}), high temperature (296.1 ± 8.02 K) and relative low RH (0.70 ± 0.12). The averaged pH value at transition period was 3.63 ± 0.27, and the AWC, excess NH_4^+, temperature, and RH were 115.1 ± 79.4 μg m^{-3}, 9.04 ± 3.67 μg m^{-3}, 286.2 ± 6.45 K and 0.80 ± 0.12, respectively. From clean to transition and polluted periods, the aerosol pH values gradually increased with the increasing of AWC, excess NH_4^+, RH and the decreasing of temperature (Figure 9). From transition to polluted periods, the aerosol pH value increased by 0.21 units, which was less than that from the clean to transition periods (by 0.56 units). However, the increasing amounts of AWC from the transition to polluted periods were higher than those from the clean to transition periods. It further verified that the effect of AWC on aerosol acidity was not linear as mentioned above.

The O_3 concentrations were the lowest in polluted periods, indicating weak photochemical activity (Wang et al., 2016a). Moreover, accompanied with high RH, aqueous reaction was the dominated atmospheric reaction in polluted periods, resulting in the increasing of SOR (sulfur oxidation rate), NOR (nitrogen oxidation rate) and AOR (ammonia conversion rate). High pH can

further accelerate the SOR, NOR and AOR rate. During the transition processes, no significant correlations were found between mineral components (Ca^{2+}, Mg^{2+}, K^{+}, and Na^{+}) and pH, implying the impact of mineral components on aerosol acidity was negligible in Wuhan.

A conceptual schematic was proposed as Figure 10 shown, along with the air quality worsened from clean to transition and to polluted situation, the fraction of second inorganic salts in $PM_{2.5}$, AWC, excess NH_4^+ and the pH of fine particles all added. Excess NH_4^+ and SNA formation showed steady growth from clean-transition-polluted. However, the AWC increase was more significant at higher polluted periods and the temperature decreasing was more obvious at lower polluted periods. The aerosol pH increasing unit from clean to transition episodes were larger than that for the pollution transformation from the transition to polluted episodes. The conceptual model comprehensively explained the role of ambient RH and temperature on the formation of SNA and AWC calculating, and furthermore the pH variation during different pollution periods.

3.5 Aerosol acidity for different origination of air masses

In the study period, there were four main directions for the air masses transported to Wuhan, namely northeast (C1), northwest (C2), south (C3) and west (C4), with the proportion of 24%, 16%, 57% and 4%, respectively (Figure 11). The aerosol acidity for C1 and C2 air masses were higher than those of C3 and C4, and associated with lower values of AWC and excess NH_4^+. The RH in southern China was always higher than those in northern China for each season (Figure 4b). Air masses from northwest mainly in winter were usually dry and saturated with small amounts of water, resulting in low pH of aerosols. More moisture air from south mainly in summer elevated aerosol pH value. Although there were minor air masses from the west to Wuhan, the pH for C4 was higher, which may be resulted from the higher AWC for C4 (Figure 11) with higher RH (Figure 4b). The amounts of excess NH_4^+ was in the order as C4 > C3 > C2≈C1, and interestingly, the pH value exhibited the similar rule, which further reflected the effect of excess NH_4^+ on aerosol acidity in Central China. Cluster analysis in this section highlighted that the current conclusions drawn from the research on aerosol acidity and its role in a typical haze formation event in North China could be not suitable for that in Wuhan, which needs a further detailed and comprehensive study, along with more chemical components investigated.

4. Conclusion

This study observed the hourly water-soluble inorganic ions from September 2015 to August

2016 in Wuhan. Thermodynamic model ISOROPPIA-Ⅱ was used to calculate the aerosol acidity. The seasonal and monthly aerosol acidity variation and its role in air pollution transition were discussed, and the possible impacting factors were identified.

The mass fraction of SNA in total water-soluble inorganic ions and $PM_{2.5}$ were 92% and 64% on average, respectively. Moderate acidic of fine particles in Wuhan was found, with the average of pH as 3.30. The aerosol acidity was higher in July, August and September and lower in January and March. The higher RH (averaged as 0.74 ± 0.13), excess ammonium (averaged as 6.06 ± 4.51 μg m^{-3}) and abundant aerosol water content (averaged as 71.0 ± 82.8 μg m^{-3}) were the key reasons for the lower aerosol acidity in Wuhan compared with other cities. At much lower AWC level (about lower than 15 μg m^{-3}), the particle pH showed a decreasing trend with AWC increased. Along with the AWC continuous increasing (> ~15 μg m^{-3}), a logarithmic correlation was found between AWC and aerosol pH. When AWC was higher than about 380 μg m^{-3}, along with the further increasing of AWC, a slowly increasing and gradually no obvious growth of pH was found. pH firstly decreased with atmospheric RH increasing at lower RH values and then increased with RH increasing, with the turning point of RH as about 0.48. Lower temperature was corresponded with higher AWC and pH, and when the temperature was higher than 303 K (about 30 ℃), more acidic aerosols were found.

There also was a logarithmic growth of particle pH with total NH_x (NH_3 + NH_4^+) increasing. Aerosol in Wuhan belonged to the stage of pH rapid growth with ammonia or ammonium increasing. It can be predicted that fine particles pH in Wuhan will continuously increase if the ammonia or ammonium was not controlled effectively, and the increasing extent will be more obvious than that in northern China. Aerosol acidity gradually decreased from clean to transition and to polluted periods. Air masses originated from northeast and northwest directions with lower AWC and excess NH_4^+ contributed to the higher acidic aerosol of Wuhan, while air masses from south and west regions exhibited lower aerosol acidity, with more AWC and excess NH_4^+ carried.

This paper firstly analyzed the aerosol pH values with a one-year high time resolution dataset at a megacity with specific location, meteorological and environmental conditions of Central China, which is meaningful for understanding the aerosol acidity and its dominated impacting factors. It also highlights the importance of controlling ammonia in Wuhan in aggravating air pollution, which is helpful for other megacities surrounded by abundant agricultural activities in the world.

Acknowledgement. This work was finically supported by the Key Program of Ministry of Science and Technology of the People's Republic of China (2016YFA0602002, 2017YFC0212602). The research was also supported by the Key project of technical innovation for the Science and Technology of Hubei Province (2017ACA089), Research Program of Environmental Protection of Hubei Province in 2017 and Fundamental Research Funds for the Central Universities, China University of Geosciences, Wuhan.

Data availability

The data can be accessed on request to the Shaofei Kong (kongshaofei@cug.edu.cn).

References:

Bian, Y. X., Zhao, C. S., Ma, N., Chen, J., and Xu, W. Y.: A study of aerosol liquid water content based on hygroscopicity measurements at high relative humidity in the North China Plain, Atmos. Chem. Phys., 14, 6417-6426, doi:10.5194/acp-14-6417-2014, 2014.

Bougiatioti, A., Nikolaou, P., Stavroulas, I., Kouvarakis, G., Weber, R., Nenes, A., Kanakidou, M., and Mihalopoulos, N.: Particle water and pH in the eastern Mediterranean: source variability and implications for nutrient availability, Atmos. Chem. Phys., 16, 4579-4591, doi:10.5194/acp-16-4579-2016, 2016.

Cao, G., and Jang, M.: An SOA Model for Toluene Oxidation in the Presence of Inorganic Aerosols, Environ. Sci. Technol., 44, 727-733, doi:10.1021/es901682r, 2010.

Carslaw, K. S., Clegg, S. L., and Brimblecombe, P.: A Thermodynamic Model of the System HCl-HNO_3-H_2SO_4-H_2O, Including Solubilities of HBr, from <200 to 328 K, J. Phys. Chem., 99, 11557-11574, doi:10.1021/j100029a039, 1995.

Chen, P., Wang, T., Dong, M., Kasoar, M., Han, Y., Xie, M., Li, S., Zhuang, B., Li, M., and Huang, T.: Characterization of major natural and anthropogenic source profiles for size-fractionated PM in Yangtze River Delta, Sci. Total Environ., 598, 135-145, doi:10.1016/j.scitotenv.2017.04.106, 2017.

Cheng, Y., Zheng, G., Wei, C., Mu, Q., Zheng, B., Wang, Z., Gao, M., Zhang, Q., He, K., Carmichael, G., Pöschl, U., and Su, H.: Reactive nitrogen chemistry in aerosol water as a source of sulfate during haze events in China, Sci. Adv., 2, doi:10.1126/sciadv.1601530, 2016.

Clegg, S. L., Brimblecombe, P., and Wexler, A. S.: Thermodynamic Model of the System H^+–NH_4^+–SO_4^{2-}–NO_3^-–H_2O at Tropospheric Temperatures, J. Phys. Chem., 102, 2137-2154, doi:10.1021/jp973042r, 1998.

Crumeyrolle, S., Gomes, L., Tulet, P., Matsuki, A., Schwarzenboeck, A., and Crahan, K.: Increase of the aerosol hygroscopicity by cloud processing in a mesoscale convective system: a case study from the AMMA campaign, Atmos. Chem. Phys., 8, 6907-6924, doi:10.5194/acp-8-6907-2008, 2008.

Engelhart, G. J., Hildebrandt, L., Kostenidou, E., Mihalopoulos, N., Donahue, N. M., and Pandis, S. N.: Water content of aged aerosol, Atmos. Chem. Phys., 11, 911-920, doi:10.5194/acp-11-911-2011, 2011.

Ervens, B., Turpin, B. J., and Weber, R. J.: Secondary organic aerosol formation in cloud droplets and aqueous particles (aqSOA): a review of laboratory, field and model studies, Atmos. Chem. Phys.,

11, 11069-11102, doi:10.5194/acp-11-11069-2011, 2011.

Fountoukis, C., and Nenes, A.: ISORROPIA II: a computationally efficient thermodynamic equilibrium model for K^+-Ca^{2+}-Mg^{2+}-NH_4^+-Na^+-SO_4^{2-}-NO_3^--Cl^--H_2O aerosols, Atmos. Chem. Phys., 7, 4639-4659, doi:10.5194/acp-7-4639-2007, 2007.

Fourtziou, L., Liakakou, E., Stavroulas, I., Theodosi, C., Zarmpas, P., Psiloglou, B., Sciare, J., Maggos, T., Bairachtari, K., Bougiatioti, A., Gerasopoulos, E., Sarda-Estève, R., Bonnaire, N., and Mihalopoulos, N.: Multi-tracer approach to characterize domestic wood burning in Athens (Greece) during wintertime, Atmos. Environ., 148, 89-101, doi:10.1016/j.atmosenv.2016.10.011, 2017.

Friese, E., and Ebel, A.: Temperature Dependent Thermodynamic Model of the System H^+–NH_4^+–Na^+–SO_4^{2-}–NO_3^-–Cl^-–H_2O, J. Phys. Chem., 114, 11595-11631, doi:10.1021/jp101041j, 2010.

Fu, X., Wang, S., Chang, X., Cai, S., Xing, J., and Hao, J.: Modeling analysis of secondary inorganic aerosols over China: pollution characteristics, and meteorological and dust impacts, Sci. Rep., 6, 35992, doi:10.1038/srep35992, 2016.

Gao, J., Wang, K., Wang, Y., Liu, S., Zhu, C., Hao, J., Liu, H., Hua, S., and Tian, H.: Temporal-spatial characteristics and source apportionment of $PM_{2.5}$ as well as its associated chemical species in the Beijing-Tianjin-Hebei region of China, Environ. Pollut., 233, 714-724, doi:10.1016/j.envpol.2017.10.123, 2018.

Grassian, V. H.: Heterogeneous uptake and reaction of nitrogen oxides and volatile organic compounds on the surface of atmospheric particles including oxides, carbonates, soot and mineral dust: Implications for the chemical balance of the troposphere, Int. Rev. in Phys. Chem., 20, 467-548, doi:10.1080/01442350110051968, 2001.

Guo, H., Xu, L., Bougiatioti, A., Cerully, K. M., Capps, S. L., Hite Jr, J. R., Carlton, A. G., Lee, S. H., Bergin, M. H., Ng, N. L., Nenes, A., and Weber, R. J.: Fine-particle water and pH in the southeastern United States, Atmos. Chem. Phys., 15, 5211-5228, doi:10.5194/acp-15-5211-2015, 2015.

Guo, H., Sullivan, A. P., Campuzano-Jost, P., Schroder, J. C., Lopez-Hilfiker, F. D., Dibb, J. E., Jimenez, J. L., Thornton, J. A., Brown, S. S., Nenes, A., and Weber, R. J.: Fine particle pH and the partitioning of nitric acid during winter in the northeastern United States, J. Geophys. Res., 121, 10,355-310,376, doi:10.1002/2016JD025311, 2016.

Johnson, A.H., Moyer, A., Bedison, J., L. Richter, S., and Andersen Willig, S.: Seven decades of

calcium depletion in organic horizons of adirondack forest soils, Soil Sci. Soc. Am. J., 72: 1824-1830, doi: 10.2136/sssaj2006.0407, 2008.

Han, X., Guo, Q., Liu, C., Fu, P., Strauss, H., Yang, J., Hu, J., Wei, L., Ren, H., Peters, M., Wei, R., and Tian, L.: Using stable isotopes to trace sources and formation processes of sulfate aerosols from Beijing, China, Sci. Rep., 6, 29958, doi: 10.1038/srep29958, 2016.

Hand, J. L., Schichtel, B. A., Malm, W. C., and Pitchford, M. L.: Particulate sulfate ion concentration and SO_2 emission trends in the United States from the early 1990s through 2010, Atmos. Chem. Phys., 12, 10353-10365, doi:10.5194/acp-12-10353-2012, 2012.

He, K., Zhao, Q., Ma, Y., Duan, F., Yang, F., Shi, Z., and Chen, G.: Spatial and seasonal variability of $PM_{2.5}$ acidity at two Chinese megacities: insights into the formation of secondary inorganic aerosols, Atmos. Chem. Phys., 12, 1377-1395, doi:10.5194/acp-12-1377-2012, 2012.

Hegde, P., Kawamura, K., Joshi, H., and Naja, M.: Organic and inorganic components of aerosols over the central Himalayas: winter and summer variations in stable carbon and nitrogen isotopic composition, Environ. Sci. Pollut. Res., 23, 6102-6118, doi:10.1007/s11356-015-5530-3, 2016.

Hennigan, C. J., Izumi, J., Sullivan, A. P., Weber, R. J., and Nenes, A.: A critical evaluation of proxy methods used to estimate the acidity of atmospheric particles, Atmos. Chem. Phys., 15, 2775-2790, doi:10.5194/acp-15-2775-2015, 2015.

Huang, X., Qiu, R., Chan, C. K., and Ravi Kant, P.: Evidence of high $PM_{2.5}$ strong acidity in ammonia-rich atmosphere of Guangzhou, China: Transition in pathways of ambient ammonia to form aerosol ammonium at $[NH_4^+]/[SO_4^{2-}] = 1.5$, Atmos. Res., 99, 488-495, doi:10.1016/j.atmosres.2010.11.021, 2011.

Huang, X., Song, Y., Li, M., Li, J., Huo, Q., Cai, X., Zhu, T., Hu, M., and Zhang, H.: A high-resolution ammonia emission inventory in China, Global Biogeochem. Cy., 26, GB1030, doi:10.1029/2011GB004161, 2012.

Huang, X., Liu, Z., Zhang, J., Wen, T., Ji, D., and Wang, Y.: Seasonal variation and secondary formation of size-segregated aerosol water-soluble inorganic ions during pollution episodes in Beijing, Atmos. Res., 168, 70-79, doi:10.1016/j.atmosres.2015.08.021, 2016.

Jang, M., Czoschke, N. M., Lee, S., and Kamens, R. M.: Heterogeneous Atmospheric Aerosol Production by Acid-Catalyzed Particle-Phase Reactions, Science, 298, 814-817, doi:10.1126/science.1075798, 2002.

Keene, W. C., Pszenny, A. A. P., Maben, J. R., Stevenson, E., and Wall, A.: Closure evaluation of size-resolved aerosol pH in the New England coastal atmosphere during summer, J. Geophys. Res., 109, D23307, doi:10.1029/2004JD004801, 2004.

Kong, S. F., Li, L., Li, X. X., Yin, Y., Chen, K., Liu, D. T., Yuan, L., Zhang, Y. J., Shan, Y. P., and Ji, Y. Q.: The impacts of firework burning at the Chinese Spring Festival on air quality: insights of tracers, source evolution and aging processes, Atmos. Chem. Phys., 15, 2167-2184, doi:10.5194/acp-15-2167-2015, 2015.

Kumar, S., and Sunder Raman, R.: Inorganic ions in ambient fine particles over a National Park in central India: Seasonality, dependencies between SO_4^{2-}, NO_3^-, and NH_4^+, and neutralization of aerosol acidity, Atmos. Environ., 143, 152-163, doi:10.1016/j.atmosenv.2016.08.037, 2016.

Lai, S., Zhao, Y., Ding, A., Zhang, Y., Song, T., Zheng, J., Ho, K. F., Lee, S.-c., and Zhong, L.: Characterization of $PM_{2.5}$ and the major chemical components during a 1-year campaign in rural Guangzhou, Southern China, Atmos. Res., 167, 208-215, doi:10.1016/j.atmosres.2015.08.007, 2016.

Larssen, T., Lydersen, E., Tang, D., He, Y., Gao, J., Liu, H., Duan, L., Seip, H. M., Vogt, R. D., Mulder, J., Shao, M., Wang, Y., Shang, H., Zhang, X., Solberg, S., Aas, W., Okland, T., Eilertsen, O., Angell, V., Li, Q., Zhao, D., Xiang, R., Xiao, J., and Luo, J.: Acid Rain in China, Environ. Sci. Technol., 40, 418-425, doi:10.1021/es0626133, 2006.

Lin, C.Q., Liu, G., Lau, A.K.H., Li, Y., Li, C.C., Fung, J.C.H., Lao, X.Q.: High-resolution satellite remote sensing of provincial $PM_{2.5}$ trends in China from 2001 to 2015, Atmos. Environ., 180, 110-116, doi:10.1016/j.atmosenv.2018.02.045, 2018.

Liu, M., Song, Y., Zhou, T., Xu, Z., Yan, C., Zheng, M., Wu, Z., Hu, M., Wu, Y., and Zhu, T.: Fine particle pH during severe haze episodes in northern China, Geophys.Res.Lett., 44, 5213-5221, doi:10.1002/2017GL073210, 2017.

Liu, X., Zhang, Y., Han, W., Tang, A., Shen, J., Cui, Z., Vitousek, P., Erisman, J. W., Goulding, K., Christie, P., Fangmeier, A., and Zhang, F.: Enhanced nitrogen deposition over China, Nature, 494, 459-462, doi:10.1038/nature11917, 2013.

Manktelow, P. T., Carslaw, K. S., Mann, G. W., and Spracklen, D. V.: The impact of dust on sulfate aerosol, CN and CCN during an East Asian dust storm, Atmos. Chem. Phys., 10, 365-382, doi:10.5194/acp-10-365-2010, 2010.

Meng, Z., Seinfeld, J. H., Saxena, P., and Kim, Y. P.: Atmospheric Gas-Aerosol Equilibrium: IV.

Thermodynamics of Carbonates, Aerosol Sci. Tech., 23, 131-154, doi:10.1080/02786829508965300, 1995.

Meng, Z. Y., Lin, W. L., Jiang, X. M., Yan, P., Wang, Y., Zhang, Y. M., Jia, X. F., and Yu, X. L.: Characteristics of atmospheric ammonia over Beijing, China, Atmos. Chem. Phys., 11, 6139-6151, doi:10.5194/acp-11-6139-2011, 2011.

Meskhidze, N., Chameides, W. L., Nenes, A., and Chen, G.: Iron mobilization in mineral dust: Can anthropogenic SO_2 emissions affect ocean productivity?, Geophys.Res.Lett., 30, 2085, doi:10.1029/2003GL018035, 2003.

Nemitz, E., Sutton, M. A., Wyers, G. P., and Jongejan, P. A. C.: Gas-particle interactions above a Dutch heathland: I. Surface exchange fluxes of NH_3, SO_2, HNO_3 and HCl, Atmos. Chem. Phys., 4, 989-1005, doi:10.5194/acp-4-989-2004, 2004.

Nenes, A., Pandis, S. N., and Pilinis, C.: ISORROPIA: A New Thermodynamic Equilibrium Model for Multiphase Multicomponent Inorganic Aerosols, Aquat. Geochem., 4, 123-152, doi:10.1023/a:1009604003981, 1998.

Ning, G., Wang, S., Ma, M., Ni, C., Shang, Z., Wang, J., and Li, J.: Characteristics of air pollution in different zones of Sichuan Basin, China, Sci. Total Environ., 612, 975-984, doi:10.1016/j.scitotenv.2017.08.205, 2018.

Pathak, R. K., Yao, X., Lau, A. K. H., and Chan, C. K.: Acidity and concentrations of ionic species of $PM_{2.5}$ in Hong Kong, Atmos. Environ., 37, 1113-1124, doi:10.1016/S1352-2310(02)00958-5, 2003.

Pathak, R. K., Louie, P. K. K., and Chan, C. K.: Characteristics of aerosol acidity in Hong Kong, Atmos. Environ., 38, 2965-2974, doi:10.1016/j.atmosenv.2004.02.044, 2004a.

Pathak, R. K., Yao, X., and Chan, C. K.: Sampling Artifacts of Acidity and Ionic Species in $PM_{2.5}$, Environ. Sci. Technol., 38, 254-259, doi:10.1021/es0342244, 2004b.

Pathak, R. K., Wu, W. S., and Wang, T.: Summertime $PM_{2.5}$ ionic species in four major cities of China: nitrate formation in an ammonia-deficient atmosphere, Atmos. Chem. Phys., 9, 1711-1722, doi:10.5194/acp-9-1711-2009, 2009.

Pathak, R. K., Wang, T., Ho, K. F., and Lee, S. C.: Characteristics of summertime $PM_{2.5}$ organic and elemental carbon in four major Chinese cities: Implications of high acidity for water-soluble organic carbon (WSOC), Atmos. Environ., 45, 318-325, doi:10.1016/j.atmosenv.2010.10.021, 2011.

Pilinis, C., Seinfeld, J. H., and Grosjean, D.: Water content of atmospheric aerosols, Atmos. Environ.,

23, 1601-1606, doi:10.1016/0004-6981(89)90419-8, 1989.

Qi, J., Zheng, B., Li, M., Yu, F., Chen, C., Liu, F., Zhou, X., Yuan, J., Zhang, Q., and He, K.: A high-resolution air pollutants emission inventory in 2013 for the Beijing-Tianjin-Hebei region, China, Atmos. Environ., 170, 156-168, doi:10.1016/j.atmosenv.2017.09.039, 2017.

Rumsey, I. C., Cowen, K. A., Walker, J. T., Kelly, T. J., Hanft, E. A., Mishoe, K., Rogers, C., Proost, R., Beachley, G. M., Lear, G., Frelink, T., and Otjes, R. P.: An assessment of the performance of the Monitor for AeRosols and GAses in ambient air (MARGA): a semi-continuous method for soluble compounds, Atmos. Chem. Phys., 14, 5639-5658, doi:10.5194/acp-14-5639-2014, 2014.

Schindler, D. W.: Effects of Acid Rain on Freshwater Ecosystems, Science, 239, 149-157, doi:10.1126/science.239.4836.149, 1988.

Seinfeld, J. H., and Pandis, S. N.: Atmospheric chemistry and physics: from air pollution to climate change, Third ed., John Wiley & Sons, Inc., Hoboken, New Jersey, 2016.

Shen, X. J., Sun, J. Y., Zhang, X. Y., Zhang, Y. M., Zhang, L., Che, H. C., Ma, Q. L., Yu, X. M., Yue, Y., and Zhang, Y. W.: Characterization of submicron aerosols and effect on visibility during a severe haze-fog episode in Yangtze River Delta, China, Atmos. Environ., 120, 307-316, doi:10.1016/j.atmosenv.2015.09.011, 2015.

Shi, G., Xu, J., Peng, X., Xiao, Z., Chen, K., Tian, Y., Guan, X., Feng, Y., Yu, H., Nenes, A., and Russell, A. G.: pH of Aerosols in a Polluted Atmosphere: Source Contributions to Highly Acidic Aerosol, Environ. Sci. Technol., 51, 4289-4296, doi:10.1021/acs.est.6b05736, 2017.

Sun, Q., and Wexler, A. S.: Modeling urban and regional aerosols—condensation and evaporation near acid neutrality, Atmos. Environ., 32, 3527-3531, doi:10.1016/S1352-2310(98)00059-4, 1998.

Surratt, J. D., Lewandowski, M., Offenberg, J. H., Jaoui, M., Kleindienst, T. E., Edney, E. O., and Seinfeld, J. H.: Effect of Acidity on Secondary Organic Aerosol Formation from Isoprene, Environ. Sci. Technol., 41, 5363-5369, doi:10.1021/es0704176, 2007.

Tai, A. P. K., Mickley, L. J., and Jacob, D. J.: Correlations between fine particulate matter ($PM_{2.5}$) and meteorological variables in the United States: Implications for the sensitivity of $PM_{2.5}$ to climate change, Atmos. Environ., 44, 3976-3984, doi:10.1016/j.atmosenv.2010.06.060, 2010.

Tanner, R. L., Olszyna, K. J., Edgerton, E. S., Knipping, E., and Shaw, S. L.: Searching for evidence of acid-catalyzed enhancement of secondary organic aerosol formation using ambient aerosol data, Atmos. Environ., 43, 3440-3444, doi:10.1016/j.atmosenv.2009.03.045, 2009.

Tao, J., Zhang, L., Cao, J., and Zhang, R.: A review of current knowledge concerning $PM_{2.5}$ chemical composition, aerosol optical properties and their relationships across China, Atmos. Chem. Phys., 17, 9485-9518, doi:10.5194/acp-17-9485-2017, 2017.

Tian, S., Pan, Y., and Wang, Y.: Ion balance and acidity of size-segregated particles during haze episodes in urban Beijing, Atmos. Res., 201, 159-167, doi:10.1016/j.atmosres.2017.10.016, 2018.

Underwood, G. M., Song, C. H., Phadnis, M., Carmichael, G. R., and Grassian, V. H.: Heterogeneous reactions of NO_2 and HNO_3 on oxides and mineral dust: A combined laboratory and modeling study, J. Geophys. Res., 106, 18055-18066, doi:10.1029/2000JD900552, 2001.

Wang, G., Zhang, R., Gomez, M. E., Yang, L., Levy Zamora, M., Hu, M., Lin, Y., Peng, J., Guo, S., Meng, J., Li, J., Cheng, C., Hu, T., Ren, Y., Wang, Y., Gao, J., Cao, J., An, Z., Zhou, W., Li, G., Wang, J., Tian, P., Marrero-Ortiz, W., Secrest, J., Du, Z., Zheng, J., Shang, D., Zeng, L., Shao, M., Wang, W., Huang, Y., Wang, Y., Zhu, Y., Li, Y., Hu, J., Pan, B., Cai, L., Cheng, Y., Ji, Y., Zhang, F., Rosenfeld, D., Liss, P. S., Duce, R. A., Kolb, C. E., and Molina, M. J.: Persistent sulfate formation from London Fog to Chinese haze, P. Natl. Acad. Sci., 113, 13630-13635, doi:10.1073/pnas.1616540113, 2016a.

Wang, G. H., Cheng, C. L., Huang, Y., Tao, J., Ren, Y. Q., Wu, F., Meng, J. J., Li, J. J., Cheng, Y. T., Cao, J. J., Liu, S. X., Zhang, T., Zhang, R., and Chen, Y. B.: Evolution of aerosol chemistry in Xi'an, inland China, during the dust storm period of 2013 - Part 1: Sources, chemical forms and formation mechanisms of nitrate and sulfate, Atmos. Chem. Phys., 14, 11571-11585, doi:10.5194/acp-14-11571-2014, 2014.

Wang, G., Zhang, F., Peng, J., Duan, L., Ji, Y., Marrero-Ortiz, W., Wang, J., Li, J., Wu, C., Cao, C., Wang, Y., Zheng, J., Secrest, J., Li, Y., Wang, Y., Li, H., Li, N., and Zhang, R.: Particle acidity and sulfate production during severe haze events in China cannot be reliably inferred by assuming a mixture of inorganic salts, Atmos. Chem. Phys. Discuss.,1-23, doi:10.5194/acp-2018-185, 2018.

Wang, H., Shi, G., Tian, M., Zhang, L., Chen, Y., Yang, F., and Cao, X.: Aerosol optical properties and chemical composition apportionment in Sichuan Basin, China, Sci. Total Environ., 577, 245-257, doi:10.1016/j.scitotenv.2016.10.173, 2017a.

Wang, H., Zhang, D., Zhang, Y., Zhai, L., Yin, B., Zhou, F., Geng, Y., Pan, J., Luo, J., Gu, B., and Liu, H.: Ammonia emissions from paddy fields are underestimated in China, Environ. Pollut., 235, 482-488, doi:10.1016/j.envpol.2017.12.103, 2018.

Wang, H. L., Qiao, L. P., Lou, S. R., Zhou, M., Ding, A. J., Huang, H. Y., Chen, J. M., Wang, Q., Tao, S. K., Chen, C. H., Li, L., and Huang, C.: Chemical composition of $PM_{2.5}$ and meteorological impact among three years in urban Shanghai, China, J. Clean. Prod., 112, 1302-1311, doi:10.1016/j.jclepro.2015.04.099, 2016b.

Wang, S., Nan, J., Shi, C., Fu, Q., Gao, S., Wang, D., Cui, H., Saiz-Lopez, A., and Zhou, B.: Atmospheric ammonia and its impacts on regional air quality over the megacity of Shanghai, China, Sci. Rep., 5, 15842, doi: 10.1038/srep15842, 2015.

Wang, Z., Pan, X., Uno, I., Li, J., Wang, Z., Chen, X., Fu, P., Yang, T., Kobayashi, H., Shimizu, A., Sugimoto, N., and Yamamoto, S.: Significant impacts of heterogeneous reactions on the chemical composition and mixing state of dust particles: A case study during dust events over northern China, Atmos. Environ., 159, 83-91, doi:10.1016/j.atmosenv.2017.03.044, 2017b.

Watson, J. G.: Visibility: Science and Regulation, J. Air Waste Manage., 52, 628-713, doi:10.1080/10473289.2002.10470813, 2002.

Weber, R. J., Guo, H., Russell, A. G., and Nenes, A.: High aerosol acidity despite declining atmospheric sulfate concentrations over the past 15 years, Nat. Geosci., 9, 282-285, doi:10.1038/ngeo2665, 2016.

Xu, L., Guo, H., Boyd, C. M., Klein, M., Bougiatioti, A., Cerully, K. M., Hite, J. R., Isaacman-VanWertz, G., Kreisberg, N. M., Knote, C., Olson, K., Koss, A., Goldstein, A. H., Hering, S. V., de Gouw, J., Baumann, K., Lee, S.-H., Nenes, A., Weber, R. J., and Ng, N. L.: Effects of anthropogenic emissions on aerosol formation from isoprene and monoterpenes in the southeastern United States, P.Natl.Acad.Sci., 112, 37-42, doi:10.1073/pnas.1417609112, 2015a.

Xu, P., Zhang, Y., Gong, W., Hou, X., Kroeze, C., Gao, W., and Luan, S.: An inventory of the emission of ammonia from agricultural fertilizer application in China for 2010 and its high-resolution spatial distribution, Atmos. Environ., 115, 141-148, doi:10.1016/j.atmosenv.2015.05.020, 2015b.

Yang, F., Tan, J., Zhao, Q., Du, Z., He, K., Ma, Y., Duan, F., Chen, G., and Zhao, Q.: Characteristics of $PM_{2.5}$ speciation in representative megacities and across China, Atmos. Chem. Phys., 11, 5207-5219, doi:10.5194/acp-11-5207-2011, 2011.

Yang, Y., Zhou, R., Wu, J., Yu, Y., Ma, Z., Zhang, L., and Di, Y. a.: Seasonal variations and size distributions of water-soluble ions in atmospheric aerosols in Beijing, 2012, J. Environ. Sci., 34, 197-205, doi:10.1016/j.jes.2015.01.025, 2015.

Yao, X., Yan Ling, T., Fang, M., and Chan, C. K.: Comparison of thermodynamic predictions for in situ pH in $PM_{2.5}$, Atmos. Environ., 40, 2835-2844, doi:10.1016/j.atmosenv.2006.01.006, 2006.

Yao, X., Ling, T. Y., Fang, M., and Chan, C. K.: Size dependence of in situ pH in submicron atmospheric particles in Hong Kong, Atmos. Environ., 41, 382-393, doi:10.1016/j.atmosenv.2006.07.037, 2007.

Yin, L., Niu, Z., Chen, X., Chen, J., Zhang, F., and Xu, L.: Characteristics of water-soluble inorganic ions in $PM_{2.5}$ and $PM_{2.5–10}$ in the coastal urban agglomeration along the Western Taiwan Strait Region, China, Environ. Sci. Pollut. R., 21, 5141-5156, doi:10.1007/s11356-013-2134-7, 2014.

Zhang, Q., Jimenez, J. L., Worsnop, D. R., and Canagaratna, M.: A Case Study of Urban Particle Acidity and Its Influence on Secondary Organic Aerosol, Environ. Sci. Technol., 41, 3213-3219, doi:10.1021/es061812j, 2007.

Zhang, Z., Gao, J., Zhang, L., Wang, H., Tao, J., Qiu, X., Chai, F., Li, Y., and Wang, S.: Observations of biomass burning tracers in $PM_{2.5}$ at two megacities in North China during 2014 APEC summit, Atmos. Environ., 169, 54-64, doi:10.1016/j.atmosenv.2017.09.011, 2017.

Zhao, Q., He, K., Rahn, K. A., Ma, Y., Jia, Y., Yang, F., Duan, F., Lei, Y., G, C., Cheng, Y., H, L., and Wang, S.: Dust storms come to Central and Southwestern China, too: implications from a major dust event in Chongqing, Atmos. Chem. Phys., 10, 2615-2630, doi:10.5194/acp-10-2615-2010, 2010.

Zheng, M., Salmon, L. G., Schauer, J. J., Zeng, L., Kiang, C. S., Zhang, Y., and Cass, G. R.: Seasonal trends in $PM_{2.5}$ source contributions in Beijing, China, Atmos. Environ., 39, 3967-3976, doi:10.1016/j.atmosenv.2005.03.036, 2005.

Zhou, M., Zhang, Y., Han, Y., Wu, J., Du, X., Xu, H., Feng, Y., and Han, S.: Spatial and temporal characteristics of $PM_{2.5}$ acidity during autumn in marine and coastal area of Bohai Sea, China, based on two-site contrast, Atmos. Res., 202, 196-204, doi:10.1016/j.atmosres.2017.11.014, 2018.

Zhou, Y., Xue, L., Wang, T., Gao, X., Wang, Z., Wang, X., Zhang, J., Zhang, Q., and Wang, W.: Characterization of aerosol acidity at a high mountain site in central eastern China, Atmos. Environ., 51, 11-20, doi:10.1016/j.atmosenv.2012.01.061, 2012.

Zhu, C.S., Cao, J.J., Tsai, C.J., Zhang, Z.S., and Tao, J.: Biomass burning tracers in rural and urban ultrafine particles in Xi'an, China, Atmos. Pollut. Res., 8, 614-618, doi:10.1016/j.apr.2016.12.011, 2017.

Atmos. Chem. Phys. Discuss., https://doi.org/10.5194/acp-2018-367
Manuscript under review for journal Atmos. Chem. Phys.
Discussion started: 25 May 2018

Atmospheric Chemistry and Physics Discussions

Table 1. Statistic of $PM_{2.5}$ and major ionic species (average ± standard deviation, μg m^{-3}) in Wuhan from September 2015 to August 2016.

	Spring	Summer	Fall	Winter	Average
$PM_{2.5}$	59.9±29.1	37.3±12.0	62.5±26.3	92.6±45.6	63.4±35.3
SO_4^{2-}	14.9±6.21	12.2±5.86	14.1±6.30	20.4±12.1	15.2±8.24
NO_3^-	16.9±9.71	5.60±4.81	10.4±6.71	25.3±14.7	14.2±11.7
NH_4^+	11.6±5.99	6.81±3.42	8.34±3.84	15.4±8.9	10.4±6.54
Ca^{2+}	0.67±0.39	0.37±0.15	0.38±0.33	0.61±0.39	0.50±0.35
Cl^-	1.62±0.65	0.94±0.41	1.05±0.66	2.87±1.25	1.56±1.07
Na^+	0.32±0.18	0.30±0.12	0.21±0.07	0.27±0.10	0.27±0.13
Mg^{2+}	0.07±0.07	0.03±0.01	0.05±0.03	0.08±0.06	0.06±0.05
K^+	0.86±0.52	0.42±0.16	0.81±0.38	1.12±0.47	0.80±0.47
Total ions	47.0±21.8	26.7±13.0	35.3±15.9	66.0±36.1	43.0±26.5
SNA*/Total ions	0.92±0.03	0.91±0.05	0.93±0.03	0.91±0.05	0.92±0.04
SNA/$PM_{2.5}$	0.73±0.16	0.67±0.18	0.55±0.17	0.62±0.11	0.64±0.17
Total ions/$PM_{2.5}$	0.80±0.17	0.73±0.19	0.59±0.18	0.69±0.11	0.70±0.19
Cation/Anion (μeq/μeq)	1.14±0.07	1.16±0.11	1.06±0.06	1.02±0.09	1.10±0.10

*: SNA= SO_4^{2-}+ NO_3^-+ NH_4^+

Atmos. Chem. Phys. Discuss., https://doi.org/10.5194/acp-2018-367
Manuscript under review for journal Atmos. Chem. Phys.
Discussion started: 25 May 2018

Atmospheric Chemistry and Physics Discussions

Table 2. Statistic of meteorological parameters and main gaseous pollutant concentrations (average ± standard deviation, μg m^{-3}) in Wuhan during September 2015 to August 2016.

Season	Spring	Summer	Fall	Winter	Average
Temp. (K)	291.4±4.4	303.6±3.9	292.3±6.6	280.7±3.2	292.2±9.0
RH (%)	73.1±13.5	74.8±9.2	75.1±11.5	74.0±16.9	74.3±12.9
HCl	0.74±0.36	1.09±0.29	0.32±0.14	0.34±0.12	0.61±0.40
HNO_2	5.11±4.05	4.24±1.77	3.48±2.26	3.44±2.56	4.07±2.83
HNO_3	2.82±1.28	3.19±0.71	1.85±1.0	1.80±0.96	2.39±1.18
NH_3	11.0±5.45	12.64±3.19	7.22±3.3	4.59±2.87	8.88±4.89
SO_2	12.8±9.3	4.7±2.9	14.7±8.1	14.5±12.8	11.9±9.6
NO_2	37.6±15.1	22.9±9.9	39.5±15.8	44.9±18.9	36.5±17.0
O_3^*	104.9±35.5	146.6±36.3	107.3±67.9	35.6±29.3	100.5±59.7
SOR	0.48±0.15	0.63±0.14	0.42±0.17	0.53±0.20	0.51±0.18
NOR	0.24±0.11	0.16±0.10	0.16±0.09	0.30±0.14	0.21±0.12
AOR	0.49±0.15	0.32±0.10	0.52±0.15	0.74±0.14	0.52±0.20

*: hourly average value was adopted.
RH: relative humidity.
SOR: sulfur oxidation rate, SOR = SO_4^{2-} / (SO_4^{2-} + SO_2) (equivalent molar concentration)
NOR: nitrogen oxidation rate, NOR = NO_3^- / (NO_3^- + NO_2) (equivalent molar concentration).
AOR: ammonia conversion rate, AOR = NH_4^+ / (NH_4^+ + NH_3) (equivalent molar concentration).

Atmos. Chem. Phys. Discuss., https://doi.org/10.5194/acp-2018-367
Manuscript under review for journal Atmos. Chem. Phys.
Discussion started: 25 May 2018

Table 3. Comparison of fine particle acidity around the world

Cities	pH	Site types	Sampling period	Sample types	Model	Reference
Hongkong [a]	-2.5~1.5	Suburban	1997-1998	Filter	E-AIM2	Yao et al., 2007
Shanghai	-0.77±0.67	Suburban	2005.5-6	Filter	E-AIM2	Pathak et al., 2009
Lanzhou	-0.38±0.64	Suburban	2006.6-7	Filter	E-AIM2	Pathak et al., 2009
Guangzhou	0.61±0.71	Suburban	2004.5	Filter	E-AIM2	Pathak et al., 2009
Beijing	-0.52±0.62	Rural	2005.6-8	Filter	E-AIM	Pathak et al., 2009
	-1~3	Urban/rural	2005.1-2006.5	Filter	E-AIM2	He et al., 2012
	5.4-6.2	Urban	2013.1	Filter	ISORROPIA-II	Cheng et al., 2016
	3.0-4.9 (average 4.2)	Urban	2015.11-12; 2016.11-12	Online	ISORROPIA-II	Liu et al., 2017
Chongqing	0~3	Urban/rural	2005.1-2006.5	Filter	E-AIM2	He et al., 2012
Mount Tai	Spring: -0.32±1.38, Summer: -0.04±1.01	Mountain	2007.3-4,6-7	Online	E-AIM2	Zhou et al., 2012
Alabama (Southeastern UAS)	0.94±0.59	Forest	2013.6.1-7.15	Online	ISORROPIA-II	Guo et al., 2015
Crete (Greece) [b]	1.25±1.14	Background	2012.6-11	Online	ISORROPIA-II	Bougiatioti et al., 2016
Egbert, On (Canada)	1~4	Rural	2012.7-9	Online	E-AIM2	Murphy et al., 2017
Wuhan	3.30±0.49	Urban	2015.9-2016.8	Online	ISORROPIA-II	This study

[a, b]: submicron particle

Atmos. Chem. Phys. Discuss., https://doi.org/10.5194/acp-2018-367
Manuscript under review for journal Atmos. Chem. Phys.
Discussion started: 25 May 2018

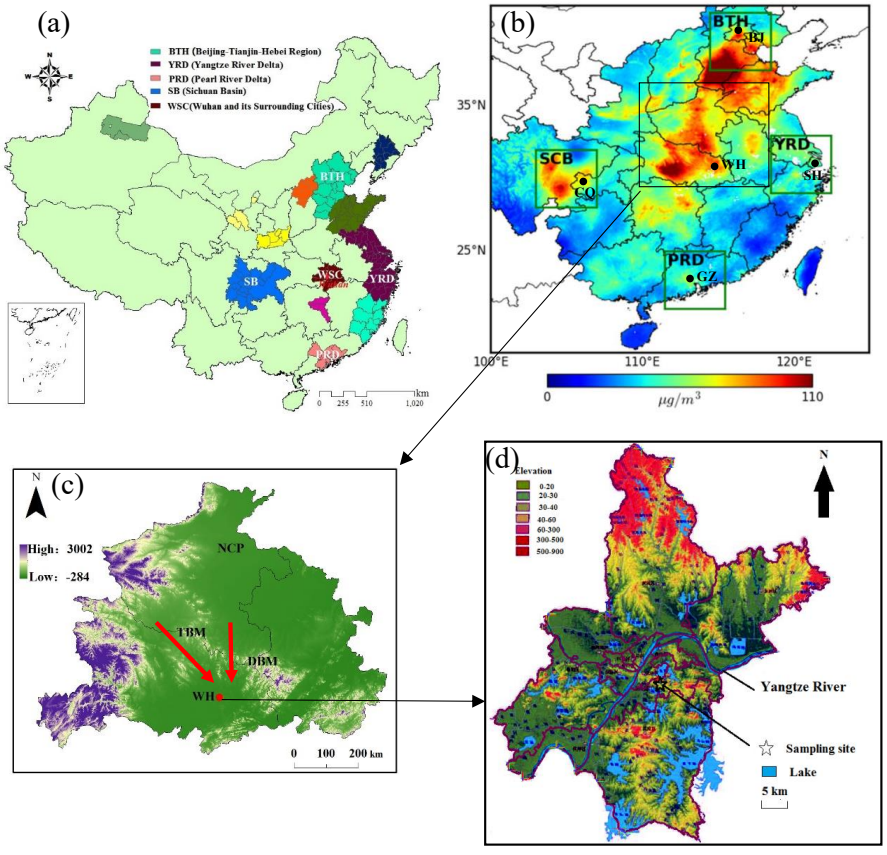

Figure 1 (a) Wuhan and its surrounding cities (WSC) belong to the key regions in the State Council's Action Plan on Prevention and Control of Atmospheric Pollution; (b) spatial distribution of the 15-year (2001-2015) mean $PM_{2.5}$ concentrations at a resolution of 1 km (Lin et al., 2018) (BTH-Beijing-Tianjin-Hebei region; YRD-Yangtze River Delta region; SCB-Sichuan Basin; PRD-Pearl River Delta region; BJ-Beijing; WH-Wuhan; SH-Shanghai; CQ-Chongqing; GZ-Guangzhou); (c) the topography of North China Plain (NCP) and surroundings of Wuhan (TBM-TongBai Mountain, DBM-Dabie Mountain). The two red lines indicate the typical transportation route of air masses in autumn and winter from NCP to Wuhan; (d) the topography of Wuhan, with the Yangtze River flowing from southwest to the northeast and abundant of lakes. The sampling site locates in the city center.

Atmos. Chem. Phys. Discuss., https://doi.org/10.5194/acp-2018-367
Manuscript under review for journal Atmos. Chem. Phys.
Discussion started: 25 May 2018

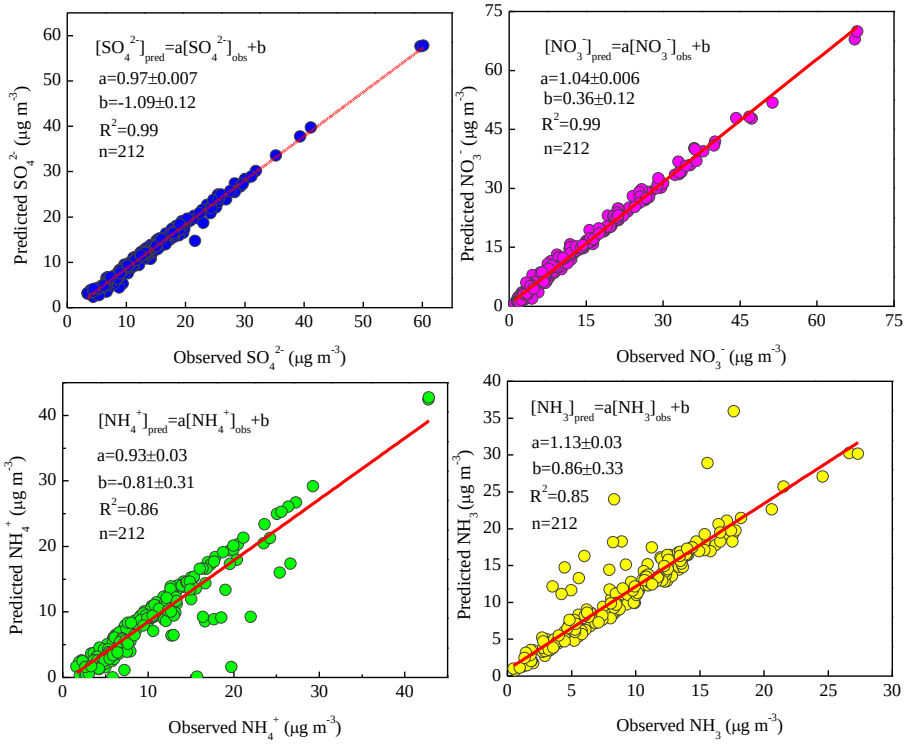

Figure 2 Comparisons of observed SO_4^{2-}, NO_3^-, NH_4^+, and NH_3 with the predicted values by ISOROPPIA-Ⅱ.

Atmos. Chem. Phys. Discuss., https://doi.org/10.5194/acp-2018-367
Manuscript under review for journal Atmos. Chem. Phys.
Discussion started: 25 May 2018

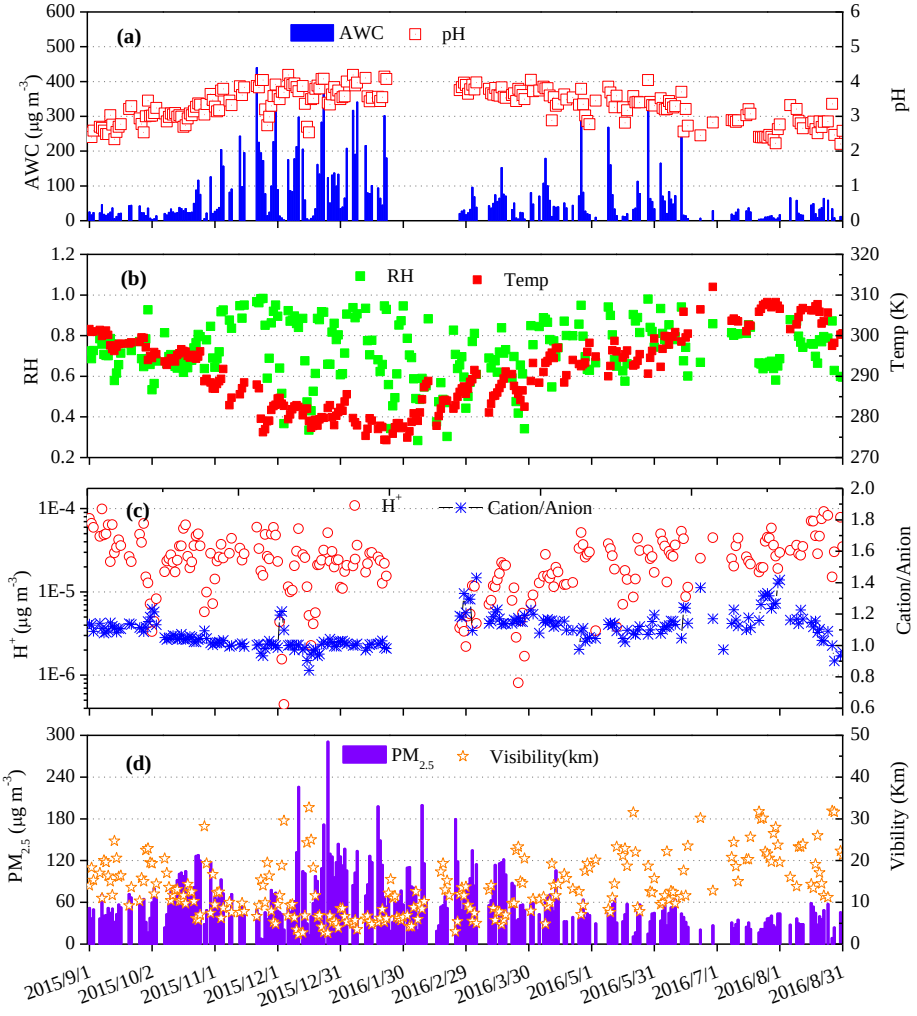

Figure 3 Daily variation of aerosol pH and AWC (a), RH and temperature (b), [H^+] and cation/anion (c), $PM_{2.5}$ concentrations and visibility (d) in Wuhan from September 2015 to August 2016.

Atmos. Chem. Phys. Discuss., https://doi.org/10.5194/acp-2018-367
Manuscript under review for journal Atmos. Chem. Phys.
Discussion started: 25 May 2018

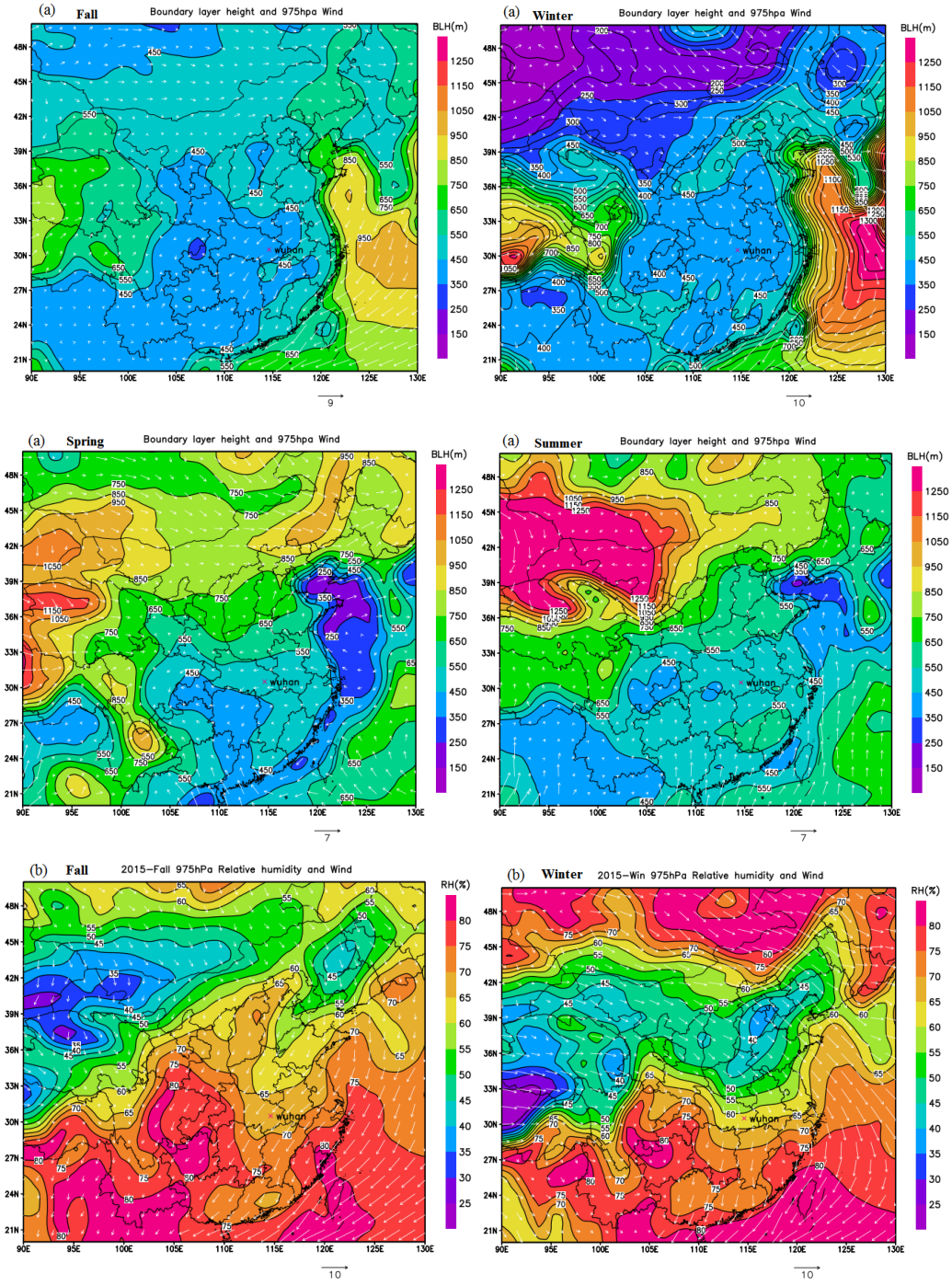

Atmos. Chem. Phys. Discuss., https://doi.org/10.5194/acp-2018-367
Manuscript under review for journal Atmos. Chem. Phys.
Discussion started: 25 May 2018

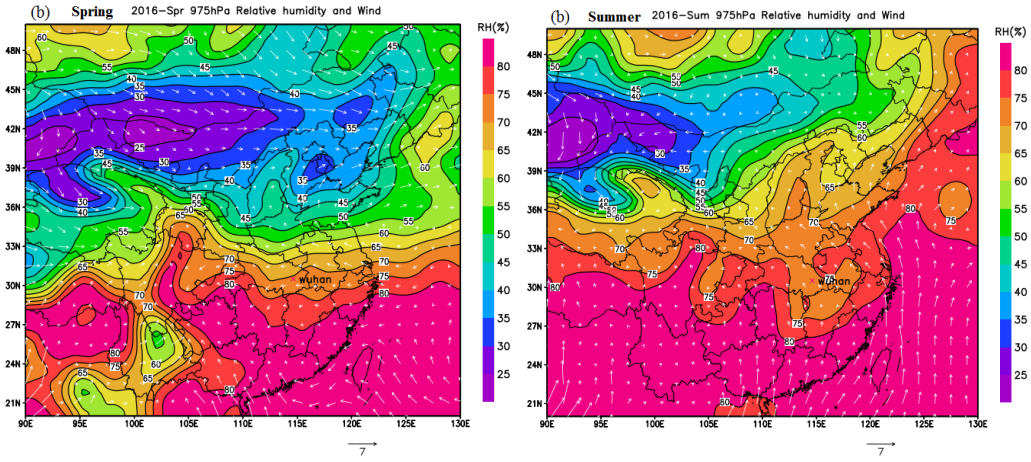

Figure 4 Atmospheric boundary layer height (a), relative humidity (b) and wind field in different seasons of Wuhan.

Atmos. Chem. Phys. Discuss., https://doi.org/10.5194/acp-2018-367
Manuscript under review for journal Atmos. Chem. Phys.
Discussion started: 25 May 2018

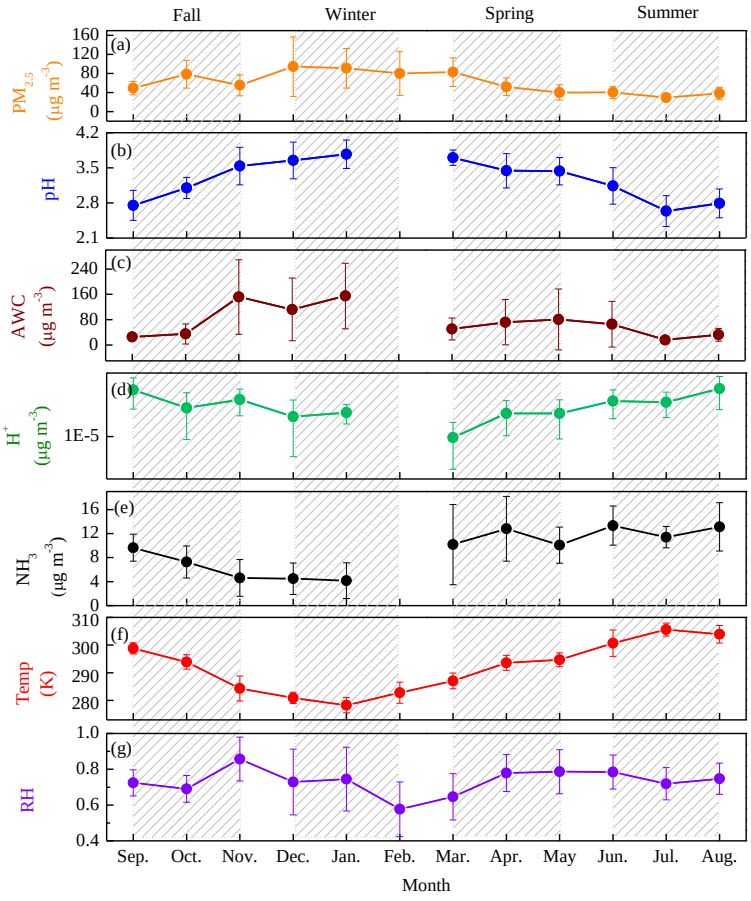

Figure 5 Monthly variation of $PM_{2.5}$ concentrations (a), pH (b), AWC (c), $[H^+]$ (d), NH_3 (e), temperature (f), RH (g) in Wuhan during September 2015 to August 2016.

Atmos. Chem. Phys. Discuss., https://doi.org/10.5194/acp-2018-367
Manuscript under review for journal Atmos. Chem. Phys.
Discussion started: 25 May 2018

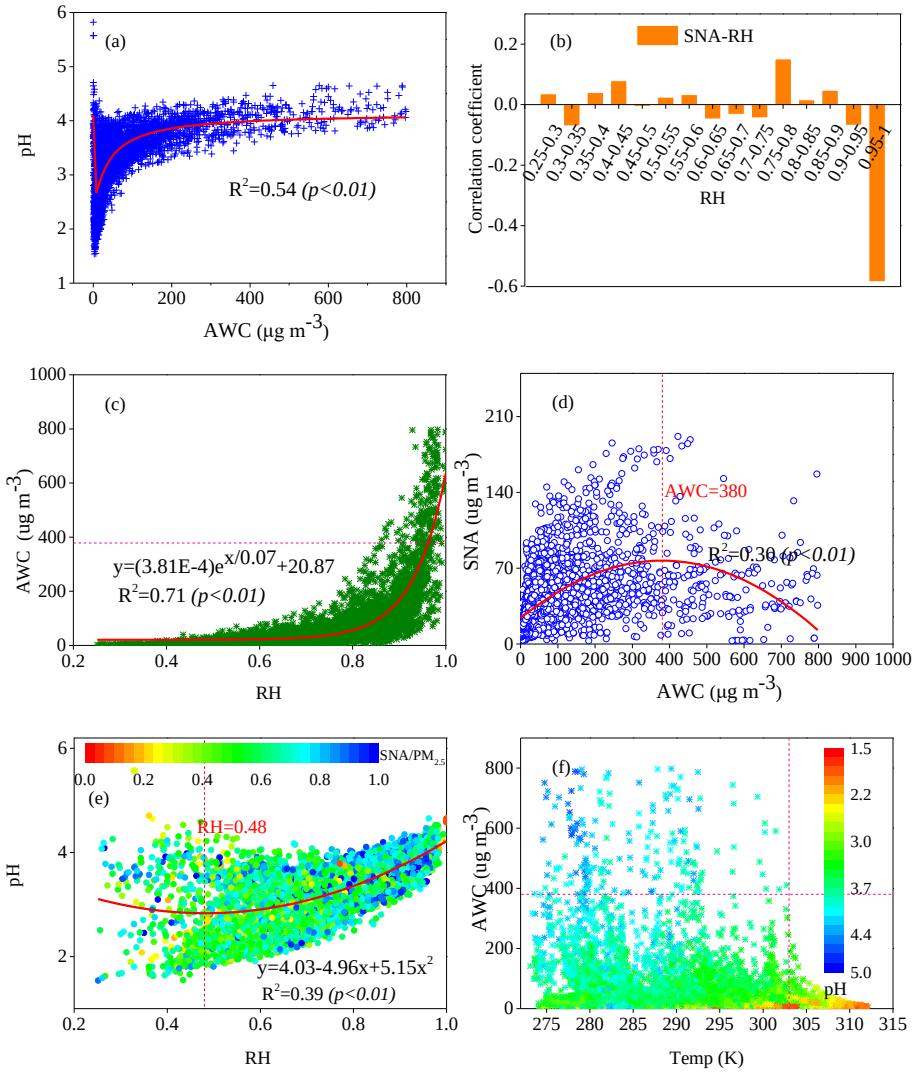

Figure 6 Relationship of pH with aerosol water content (AWC) (a), SNA-RH correlation coefficient with RH (b), AWC with RH (c), SNA with AWC (d), pH with RH (e), AWC with temperature (f) in Wuhan.

Atmos. Chem. Phys. Discuss., https://doi.org/10.5194/acp-2018-367
Manuscript under review for journal Atmos. Chem. Phys.
Discussion started: 25 May 2018

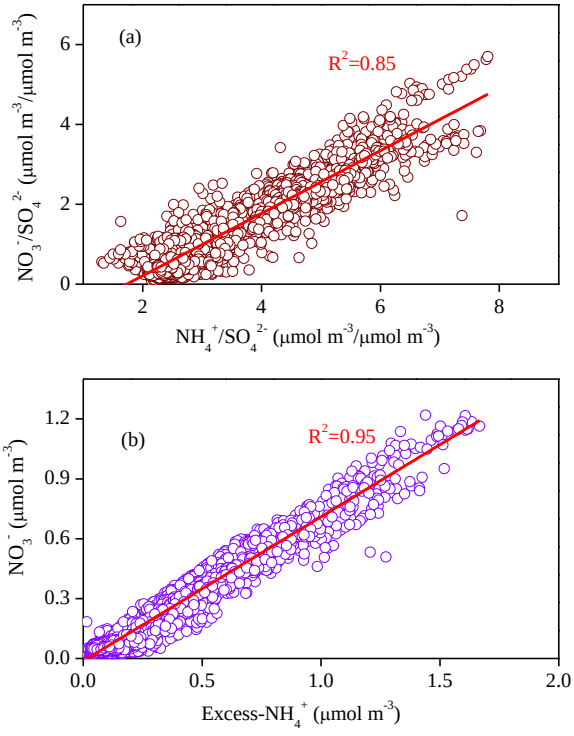

Figure 7 Relationship of NO_3^-/SO_4^{2-} with NH_4^+/SO_4^{2-} (a) and NO_3^- with excess-NH_4^+ (b).

Atmos. Chem. Phys. Discuss., https://doi.org/10.5194/acp-2018-367
Manuscript under review for journal Atmos. Chem. Phys.
Discussion started: 25 May 2018

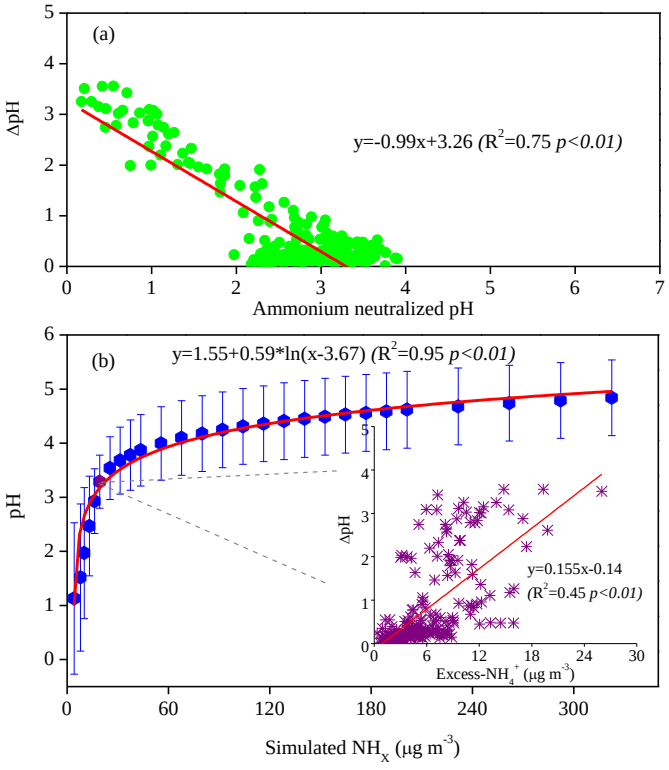

Figure 8 Relationship of pH changes (pH changes between presence and absence of excess NH_4^+) with ammonium neutralized pH (with no excess NH_4^+ case) (a); pH with simulated NH_x ($NH_x = NH_3 + NH_4^+$) (b), the special purple point in the logarithmic curve was the current state in Wuhan.

Atmos. Chem. Phys. Discuss., https://doi.org/10.5194/acp-2018-367
Manuscript under review for journal Atmos. Chem. Phys.
Discussion started: 25 May 2018

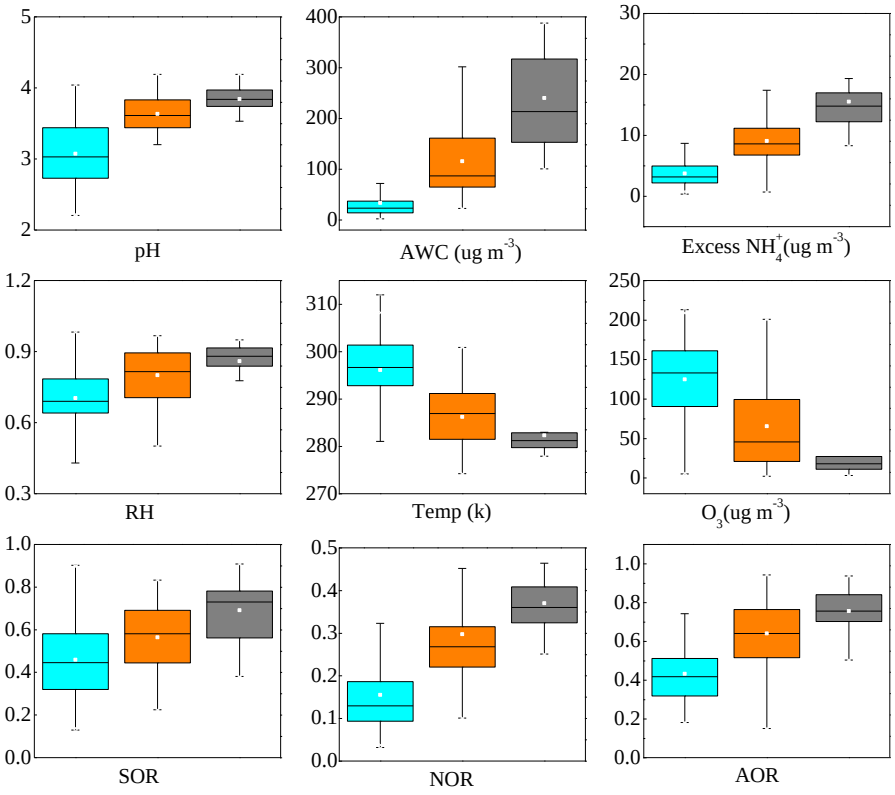

Figure 9 The pH, water content, excess NH_4^+, meteorological parameters, ozone concentration, SOR (sulfur oxidation rate), NOR (nitrogen oxidation rate) and AOR (ammonia conversion rate) in different pollution episodes. The grey, orange and blue colors indicated the polluted (visibility less than 5 km), transition (visibility 5-10 km) and clean (visibility higher than 10 km) episodes, with the average $PM_{2.5}$ concentrations of 130, 80 and 42 μg m^{-3}, respectively. The white dot in the box marks the mean value. The bottom and top vertical line correspond to the 5th and 95th percentiles, respectively. The bottom, middle and top of the horizontal lines of each box represent the 25th, 50th, and 75th percentiles of the data.

Atmos. Chem. Phys. Discuss., https://doi.org/10.5194/acp-2018-367
Manuscript under review for journal Atmos. Chem. Phys.
Discussion started: 25 May 2018

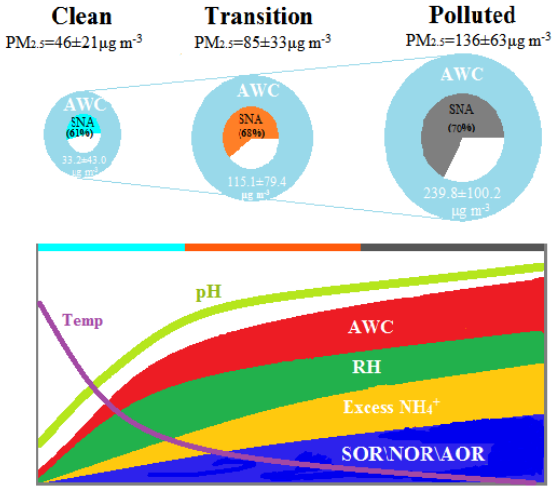

Figure 10 A conceptual schematic for the variations of fine particle mass concentrations and the driving factors impacted on aerosol pH along with the pollution aggravation.

Atmos. Chem. Phys. Discuss., https://doi.org/10.5194/acp-2018-367
Manuscript under review for journal Atmos. Chem. Phys.
Discussion started: 25 May 2018

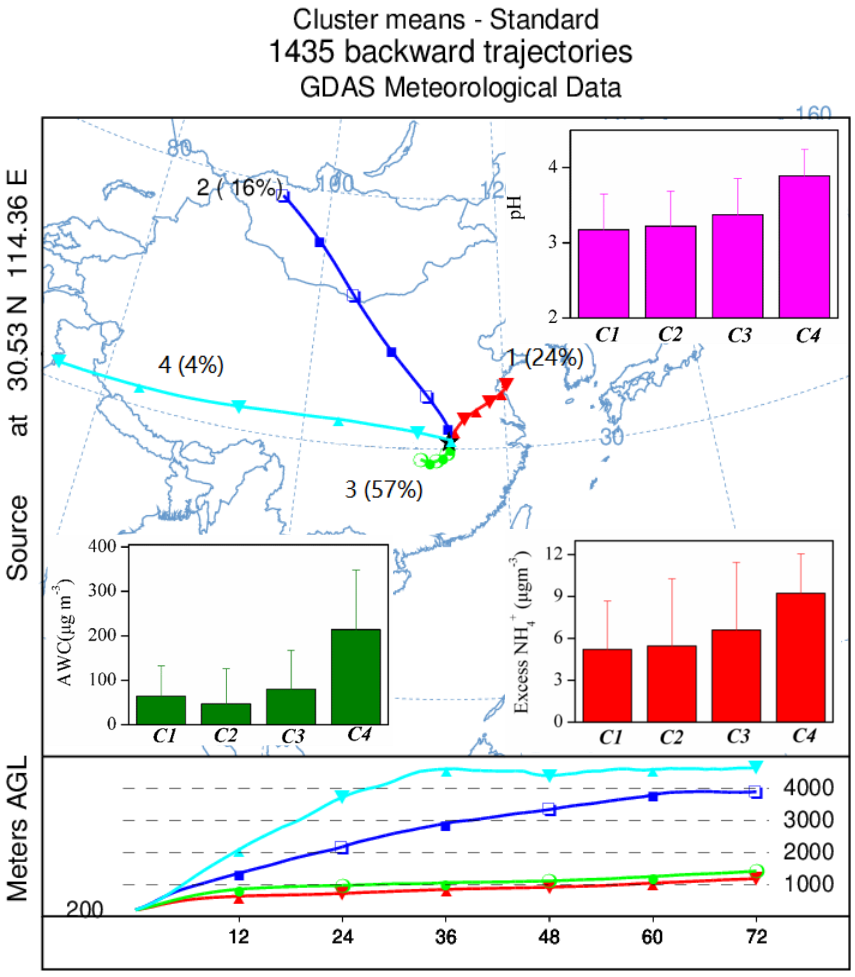

Figure 11 Backward trajectories for each cluster and corresponding pH, water content and excess NH_4^+.